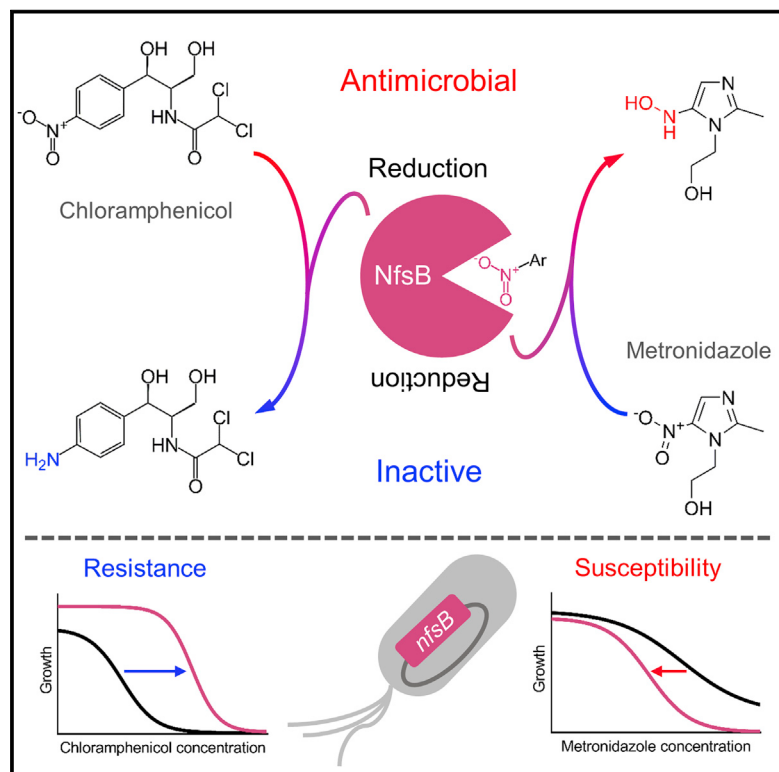


Cell Chemical Biology

Discovery and Characterization of a Nitroreductase Capable of Conferring Bacterial Resistance to Chloramphenicol

Graphical Abstract



Authors

Terence S. Crofts, Pratyush Sontha,
Amber O. King, ..., Nicole Zanolli,
John Gaumnitz, Gautam Dantas

Correspondence

tcrofts@northwestern.edu (T.S.C.),
dantas@wustl.edu (G.D.)

In Brief

Crofts et al. report the characterization of bacterial genes that confer chloramphenicol resistance by nitroreduction. The most effective gene, *H. influenzae nfsB*, encodes an enzyme that efficiently reduces the chloramphenicol nitro group *in vitro*. The authors found that resistance via reduction could be countered using the anaerobic antibiotic metronidazole.

Highlights

- Bacteria can resist chloramphenicol via reduction, but the causal genes are unknown
- nfsB* nitroreductase expression can confer chloramphenicol resistance in *E. coli*
- H. influenzae* NfsB quickly reduces chloramphenicol to amino-chloramphenicol *in vitro*
- Metronidazole potentiates chloramphenicol activity against nitro reducing *E. coli*

Discovery and Characterization of a Nitroreductase Capable of Conferring Bacterial Resistance to Chloramphenicol

Terence S. Crofts,^{1,2,5,*} Pratyush Sontha,² Amber O. King,² Bin Wang,^{1,2} Brent A. Biddy,² Nicole Zanolli,² John Gaumnitz,² and Gautam Dantas^{1,2,3,4,6,*}

¹Department of Pathology and Immunology, Washington University in St Louis School of Medicine, Saint Louis, MO 63110, USA

²The Edison Family Center for Genome Sciences and Systems Biology, Washington University in St Louis School of Medicine, Saint Louis, MO 63110, USA

³Department of Molecular Microbiology, Washington University in St Louis School of Medicine, Saint Louis, MO 63110, USA

⁴Department of Biomedical Engineering, Washington University in St Louis, Saint Louis, MO 63110, USA

⁵Present address: Department of Molecular Biosciences, Northwestern University, Evanston, IL 60208, USA

⁶Lead Contact

*Correspondence: tcrofts@northwestern.edu (T.S.C.), dantas@wustl.edu (G.D.)

<https://doi.org/10.1016/j.chembiol.2019.01.007>

SUMMARY

Widespread antibiotic resistance has led to the reappraisal of abandoned antibiotics including chloramphenicol. However, enzyme(s) underlying one form of chloramphenicol resistance, nitroreduction, have eluded identification. Here we demonstrate that expression of the *Haemophilus influenzae* nitroreductase gene *nfsB* confers chloramphenicol resistance in *Escherichia coli*. We characterized the enzymatic product of *H. influenzae* NfsB acting on chloramphenicol and found it to be amino-chloramphenicol. Kinetic analysis revealed reduction of diverse substrates including the incomplete reduction of 5-nitro antibiotics metronidazole and nitrofurantoin, likely resulting in activation of these antibiotic pro-drugs to their cytotoxic forms. We observed that expression of the *H. influenzae* *nfsB* gene in *E. coli* results in significantly increased susceptibility to metronidazole. Finally, we found that in this strain metronidazole attenuates chloramphenicol resistance synergistically, and *in vitro* metronidazole weakly inhibits chloramphenicol reduction by NfsB. Our findings reveal the underpinnings of a chloramphenicol resistance mechanism nearly 70 years after its description.

INTRODUCTION

Antibiotic resistance is a growing threat to modern medicine and is expected to be responsible for an increasing number of deaths worldwide in the future (O'Neil, 2014). Compounding this threat is the ubiquity of cryptic resistance mechanisms present in the environment (Crofts et al., 2017) and the declining development of new antibiotics (Kinch et al., 2014; Payne et al., 2007; Pye et al., 2017). One solution to this problem has been to reconsider

the use of antibiotics previously abandoned due to compromised safety or efficacy profiles (Wright, 2017). In particular, the rise of resistance specifically to β -lactams, the most widely used class of antimicrobials worldwide, has changed the cost-benefit analysis for multiple other classes of antibiotics that were formerly concluded to be too toxic for general use. For example, colistin and daptomycin are now important clinical antibiotics of last resort despite prior abandonment due to toxicity issues. Their potential toxicity is outweighed by the lethality of otherwise virtually pan-resistant infections (Čivljak et al., 2014; Li et al., 2006; The Pew Charitable Trusts, 2016; Wright, 2017). It has been suggested that amphenicols, antibiotics such as chloramphenicol (Figure 1A), thiamphenicol, and florfenicol, which have lost or failed to gain approval for human use due to potential toxicity, may follow this same path for readoption (Čivljak et al., 2014; Dinos et al., 2016; Rahim et al., 2015).

Chloramphenicol (Figure 1A), co-discovered and marketed by Parke-Davis beginning in the 1940s, is a natural product antibiotic produced by the bacterium *Streptomyces venezuelae* with antibiotic activity against Gram-positive and Gram-negative bacteria (Ehrlich et al., 1947; Smith et al., 1948). It is stable under a range of conditions (Ehrlich et al., 1947) and was the first natural product antibiotic to be economically produced synthetically (Ehrlich et al., 1947; Schwarz et al., 2004; Wright et al., 2014). Chloramphenicol is orally available and can cross the blood-brain barrier and other sites that are difficult to reach, making it a potent therapy for bacterial meningitis and tissue infections (Dinos et al., 2016; Schwarz et al., 2004).

Despite their attractiveness as antibiotics, the clinical use of amphenicols has largely ceased in more economically developed countries as a result of chloramphenicol's epidemiological linkage to hematological toxicity (Shu et al., 1987; Wallerstein et al., 1969). Potentially because of this, chloramphenicol remains active against a variety of bacterial pathogens. While chloramphenicol does not show greater efficacy against routine infections compared with current standard treatments, its use may be justifiable against multi-drug resistance organisms (Eliakim-Raz et al., 2015) as chloramphenicol retains substantial activity against Gram-positive organisms, especially methicillin-resistant

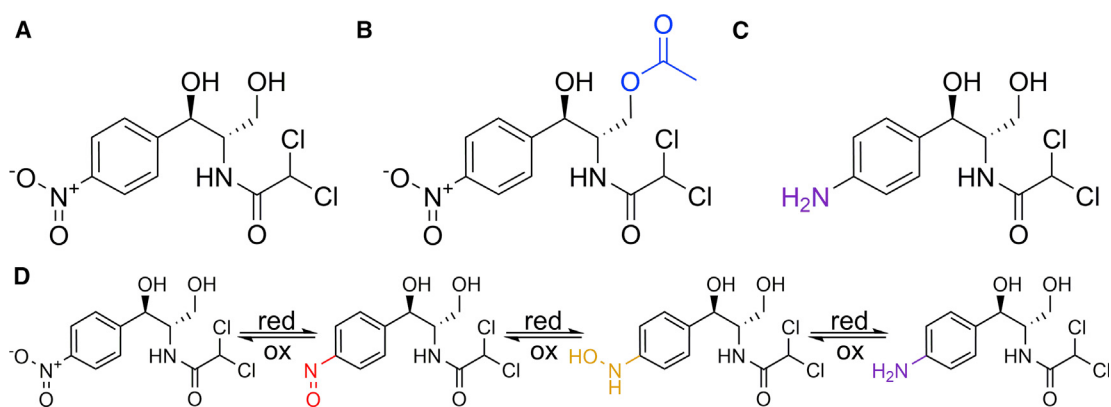


Figure 1. Structure of Chloramphenicol and Its Bacterial Modifications

(A–C) Chemical structure of (A) chloramphenicol, (B) chloramphenicol inactivated following acetylation, and (C) chloramphenicol inactivated following nitroreduction.

(D) Products of stepwise chloramphenicol reduction, from left to right: chloramphenicol, nitroso-chloramphenicol, hydroxylamino-chloramphenicol, and amino-chloramphenicol.

Staphylococcus aureus in more developed countries, and moderate activity against Gram-negative organisms (Čivljak et al., 2014; Lim et al., 2016; Nitzan et al., 2010; Sood, 2016).

The most widespread chloramphenicol resistance mechanisms are via well-annotated functions such as enzymatic inactivation (e.g., via chloramphenicol acetyltransferase, Figure 1B), efflux pump removal, and ribosome protection (Dinos et al., 2016; Long et al., 2006; Schwarz et al., 2004). One of the first reports of bacterial modification of chloramphenicol came only two years after its discovery. The authors described multiple species of bacteria, including *Escherichia coli*, having the ability to fully reduce the nitro group of chloramphenicol and in this way resist its bacteriostatic effects (Smith and Worrel, 1949). The resulting compound, amino-chloramphenicol (Figure 1C), lacked antibacterial activity, an observation borne out by studies demonstrating the importance of an electron-withdrawing constituent at this position of the molecule (Dinos et al., 2016). Since this first observation, additional studies have replicated the finding that a variety of bacteria can reduce the nitro group of chloramphenicol, resulting in altered susceptibility (Egami et al., 1951; Merkel and Steers, 1953; O'Brien and Morris, 1971; Onderdonk et al., 1979; Smith and Worrel, 1950, 1953; Smith et al., 2007). While many of these bacteria demonstrated a susceptible phenotype *in vitro*, there is evidence that in a host this strategy leads to phenotypic resistance in the presence of serum chloramphenicol concentrations reaching almost 3-fold the *in vitro* minimal inhibitory concentration (MIC) (Onderdonk et al., 1979). Furthermore, based on the phylogenetic distribution of these taxa, chloramphenicol nitroreduction is likely not limited to these individually studied organisms. Similarly, amino-chloramphenicol has been detected in the feces of conventional rats, but not in their germ-free counterparts (Glazko et al., 1952; Wal et al., 1983), and this metabolite has been documented in samples from dogs, non-human primates, and humans as well (Glazko, 1987a; Holt et al., 1995; Kunin et al., 1959). Despite its apparent ubiquity and potential medical importance, the mechanism underlying chloramphenicol reduction has never been described and no genes or enzymes having this activity have been documented.

We set out to identify bacterial genes that may be effectors of this activity. The oxygen-insensitive family of nitroreductases, such as those encoded by the *nfsA* or *nfsB* genes in *E. coli*, are known to be promiscuous reducers of aromatic nitro groups, and homologs of these genes are found across diverse bacterial taxa, including in many members of the intestinal microbiome (Roldán et al., 2008). Nitro-reduction via these enzymes occurs two electrons at a time, often stopping at the production of a hydroxylamino group after a four-electron reduction (Roldán et al., 2008), though some enzymes, such as the NfsB homologs from *E. coli*, *Enterobacter cloacae*, and *Salmonella enterica*, have been demonstrated to reduce aromatic nitro groups completely to amines (LinWu et al., 2009; Yanto et al., 2010) (Figure 1D). We found that expression of some of these genes in *E. coli* led to altered susceptibility/resistance to chloramphenicol. *In vitro* characterization of the enzyme corresponding to the most active gene, the *Haemophilus influenzae nfsB* homolog, revealed an ability to reduce chloramphenicol to amino-chloramphenicol, as well as an ability to at least partially reduce several other aromatic nitro-substrates. Finally, we made initial strides into countering this cryptic resistance mechanism, showing that the commonly used antibiotic metronidazole both inhibits chloramphenicol reduction *in vitro* and synergistically kills chloramphenicol-reducing *E. coli* in the presence of chloramphenicol. We report the isolation and characterization of genes/enzymes that confer chloramphenicol resistance via a reductive mechanism and consider the implications of our findings for future amphenicol use in the clinic, as well as potential links to chloramphenicol toxicity.

RESULTS

Nitroreductase Gene Expression Can Alter *E. coli* Chloramphenicol Susceptibility

In choosing which candidate genes to assay for chloramphenicol reduction activity, we began our search by focusing (fortuitously) on homologs of the oxygen-insensitive type I nitroreductase family. We choose to focus at first on oxygen-insensitive

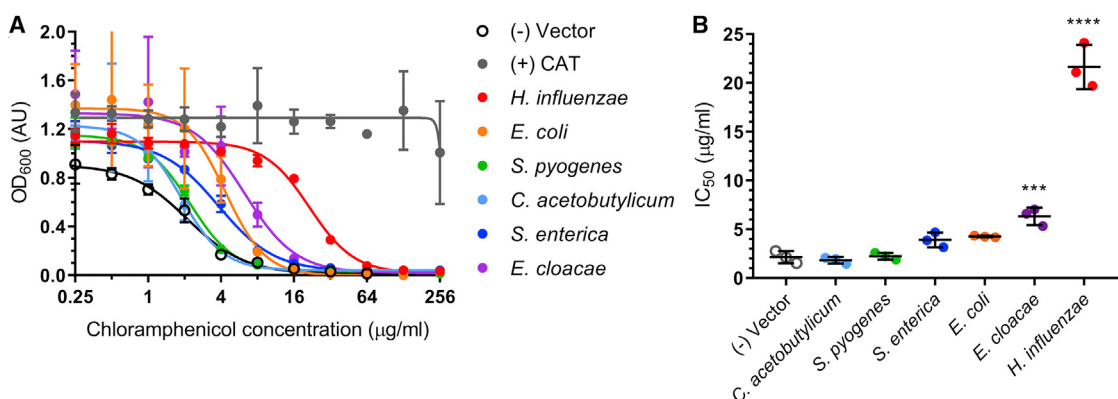


Figure 2. Reductase Expression Can Alter Susceptibility of *E. coli* to Chloramphenicol

(A and B) Dose-response curves of microbroth dilution assays for *E. coli* expressing predicted reductase gene homologs in the presence of chloramphenicol (A) with corresponding 50% inhibitory concentrations (IC_{50}) calculated from the curve fit (B). All points are averages of triplicate experiments with standard deviation (SD) error bars. Statistical significance was calculated with respect to the vector control by ordinary one-way ANOVA with Dunnett's correction for multiple comparisons. Adjusted p value is displayed as *** $p \leq 0.0001$ and ** $p < 0.001$. CAT, chloramphenicol acetyltransferase.

enzymes due to the ability of this class to reduce aromatic nitro groups to a stable amino product, rather than to unstable intermediates as has been observed with many type II oxygen-sensitive enzymes (Roldán et al., 2008). The most relevant members of this class of enzyme are the well-studied *E. coli* NfsA and NfsB enzymes (Zenno et al., 1996a, 1996b). Because a *Lactococcus lactis* homolog of *E. coli* NfsA (CinD) has been reported to be unable to reduce chloramphenicol *in vitro* (Mermod et al., 2010), we further chose to focus on predicted NfsB homologs originating from bacterial taxa that have been phenotypically associated with chloramphenicol reduction (Table S1) including *E. coli*, *S. enterica*, *E. cloacae*, *H. influenzae*, *Clostridium acetobutylicum*, and *Streptococcus pyogenes*. We cloned a target gene from each organism into a constitutive expression vector for expression in *E. coli*. Because amino-chloramphenicol (Figure 1C) does not show antibacterial properties (Smith and Worrel, 1949; Smith et al., 2007), we utilized microbroth dilution susceptibility testing to determine whether any of the strains showed altered susceptibility to chloramphenicol as a result of reductase expression (Figure 2A). Our negative control, *E. coli* carrying an empty vector, was susceptible to chloramphenicol, with a calculated 50% inhibitory concentration (IC_{50}) of $2.12 \pm 0.19 \mu\text{g}/\text{mL}$ (Figure 2B) and an observed MIC of $8 \mu\text{g}/\text{mL}$ across three replicates. *E. coli* expressing a canonical chloramphenicol resistance gene, chloramphenicol acetyltransferase or cat (Schwarz et al., 2004), was highly resistant with an $\text{IC}_{50}/\text{MIC}$ greater than $256 \mu\text{g}/\text{mL}$. Two of the cloned reductases imparted a significant increase in chloramphenicol resistance, as measured by IC_{50} , when expressed in *E. coli*: the nfsB homologs from *H. influenzae* ($\text{IC}_{50} 21.5 \pm 1.1 \mu\text{g}/\text{mL}$) and *E. cloacae* ($\text{IC}_{50} 6.24 \pm 1.1 \mu\text{g}/\text{mL}$) (Figure 2B). *E. coli* strains expressing these genes were also the only strains to show at least a two-step jump in MIC compared with vector control, with the *H. influenzae* nfsB-expressing strain showing growth up to $64 \mu\text{g}/\text{mL}$ chloramphenicol, and the *E. cloacae* nfsB-expressing strain showing growth up to $32 \mu\text{g}/\text{mL}$ chloramphenicol.

Because we observed variation in the ability of nfsB expression to confer resistance to chloramphenicol, we set out to

determine whether activity could be predicted by amino acid sequence. We focused on the amino acid sequences of the six reductases tested in *E. coli* (Figure 2), two other well-studied nitroreductases (*E. coli* NfsA [Zenno et al., 1996a] and *L. lactis* CinD [Mermod et al., 2010]), and nine sequences corresponding to nfsB homologs from bacterial taxa previously tested for their ability to reduce chloramphenicol in culture (Smith et al., 2007). For a broader comparison, a selection of bacterial proteins annotated in UniProt as NfsB homologs were compared as well. The resulting maximum-likelihood tree (Figure 3) is organized largely by phylogeny but with evidence for clustering by function as well.

This is evident in the clustering of the Pasteurellales family, where *Haemophilus*, *Neisseria*, and *Pasteurella* genera appear to cluster as a group by phylogeny. Within this group, the *Neisseria* NfsB homologs cluster with *Haemophilus* NfsB homologs while the *Pasteurella* homolog is further removed despite its closer phylogenetic relatedness to *Haemophilus*. This subgrouping instead matches predicted ability to reduce chloramphenicol based on previous phenotypic studies (Smith et al., 2007). On the other hand, the *E. cloacae* NfsB clusters with its phylogenetic relatives, *E. coli* and *S. enterica*, although it appears to have significantly greater chloramphenicol reduction activity (Figure 2). Because our analyses did not establish any sequence markers for predicting chloramphenicol reduction, we chose to focus on further characterizing the *H. influenzae* NfsB homolog, the reductase with greatest apparent activity.

Chloramphenicol-Reducing *E. coli* Cultures Can Degrade Chloramphenicol to Non-inhibitory Levels and Rescue Susceptible Strains

One report of chloramphenicol reduction occurring in the context of a rat infection model noted the survival of susceptible bacteria despite chloramphenicol treatment with confirmed serum levels well above their MIC (Onderdonk et al., 1979). To test our system for this phenotype, we performed a series of experiments on the *E. coli* strain expressing the *H. influenzae* nfsB

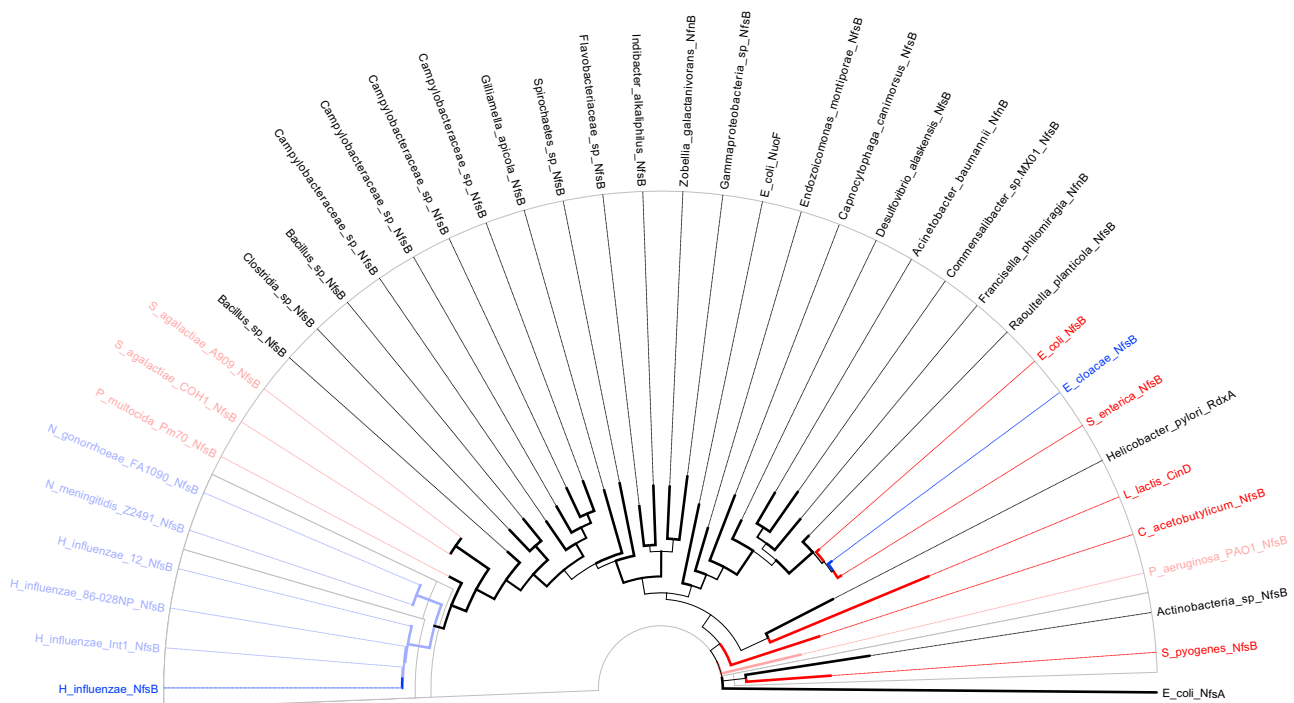


Figure 3. Phylogenetic and Amino Acid Analysis of Chloramphenicol Reducing and Non-reducing NfsB Homologs

Maximum-likelihood tree with bootstrap support (100 tests, indicated by branch thickness) of predicted NfsB homologs. Solid blue branches/taxa are those with direct evidence of chloramphenicol reduction (this paper). Light-blue and light-red branches/taxa are those with indirect evidence for or against, respectively, chloramphenicol reduction (reduction observed or not observed in native host, Smith et al., 2007). Solid red branches/taxa are those with direct evidence against chloramphenicol reduction (this paper and *L. lactis* CinD from Mermod et al., 2010).

gene. Our first approach used a chloramphenicol challenge assay in which we measured culture lag-phase duration in the presence of increasing concentrations of chloramphenicol. The utility of this lag-phase assay has previously been demonstrated for chloramphenicol (Tao et al., 2012). We observed that while our control *E. coli* strain did not show substantial growth in the presence of any concentration of chloramphenicol (Figure 4A), the *H. influenzae* *nfsB*-expressing strain grew at several concentrations (Figure 4B), in line with previous observations of chloramphenicol reduction. We found a clear correlation between the time it took the resistant strain to reach half-maximal growth and the chloramphenicol concentration in the medium (Figure 4C). In a second assay, we cultured *E. coli* containing an empty vector or a vector expressing *H. influenzae* *nfsB* in inhibitory concentrations of chloramphenicol. After removing cells, this pre-conditioned medium was assayed for its ability to support the growth of a chloramphenicol-susceptible *E. coli* strain. Both pre-conditioned medium from the empty vector *E. coli* strain and fresh medium containing chloramphenicol inhibited growth of the susceptible *E. coli* strain, while pre-conditioned medium lacking chloramphenicol supported robust growth (Figure 4D). Medium with chloramphenicol but pre-conditioned by the *H. influenzae* *nfsB*-expressing *E. coli* strain was capable of supporting significant growth, reaching approximately half the cell density as chloramphenicol-free medium, suggesting that chloramphenicol levels had been reduced from 8 µg/mL to a concentration near 2 µg/mL, the approximate IC₅₀ of the susceptible strain.

H. influenzae NfsB Reduction of Chloramphenicol Produces Amino-Chloramphenicol

Because reduction of aromatic nitro groups can result in formation of fully reduced or partially reduced products, we next sought to characterize the degree of chloramphenicol reduction by *H. influenzae* NfsB. The ability of *E. coli* expressing *H. influenzae* *nfsB* to resist chloramphenicol (Figure 2) and rescue susceptible strains (Figure 4D), suggests complete reduction of the nitro group to an amine as partially reduced intermediates could potentially spontaneously oxidize back to chloramphenicol in a futile cycle (Dingsdag and Hunter, 2018; Roldán et al., 2008). We therefore set out to characterize the *H. influenzae* NfsB chloramphenicol product *in vitro*. We cloned the *H. influenzae* *nfsB* gene into an inducible system for heterologous expression and purification in *E. coli*. After optimization (Figure S1A) we obtained an enzyme of the expected denatured size of ~25 kDa (Figure S1B). We found that *H. influenzae* NfsB (UniProt: Q57431) requires NADPH as a cofactor and does not utilize NADH (Figure S2A) and tightly binds a flavin cofactor, most likely flavin mononucleotide (FMN) (Figure S2B). The enzyme shows activity across a wide range of pH values, with highest activity recorded between pH 6.5 and pH 9 (Figure S2C), and shows activity in our assay at temperatures between 25°C and 55°C (Figure S2D). Based on these results, assays were performed at 25°C in 50 mM Tris-HCl buffer at pH 8 with NADPH and FMN.

To determine whether chloramphenicol is reduced completely to amino-chloramphenicol, we utilized liquid chromatography coupled with mass spectrometry (LC-MS). We first verified

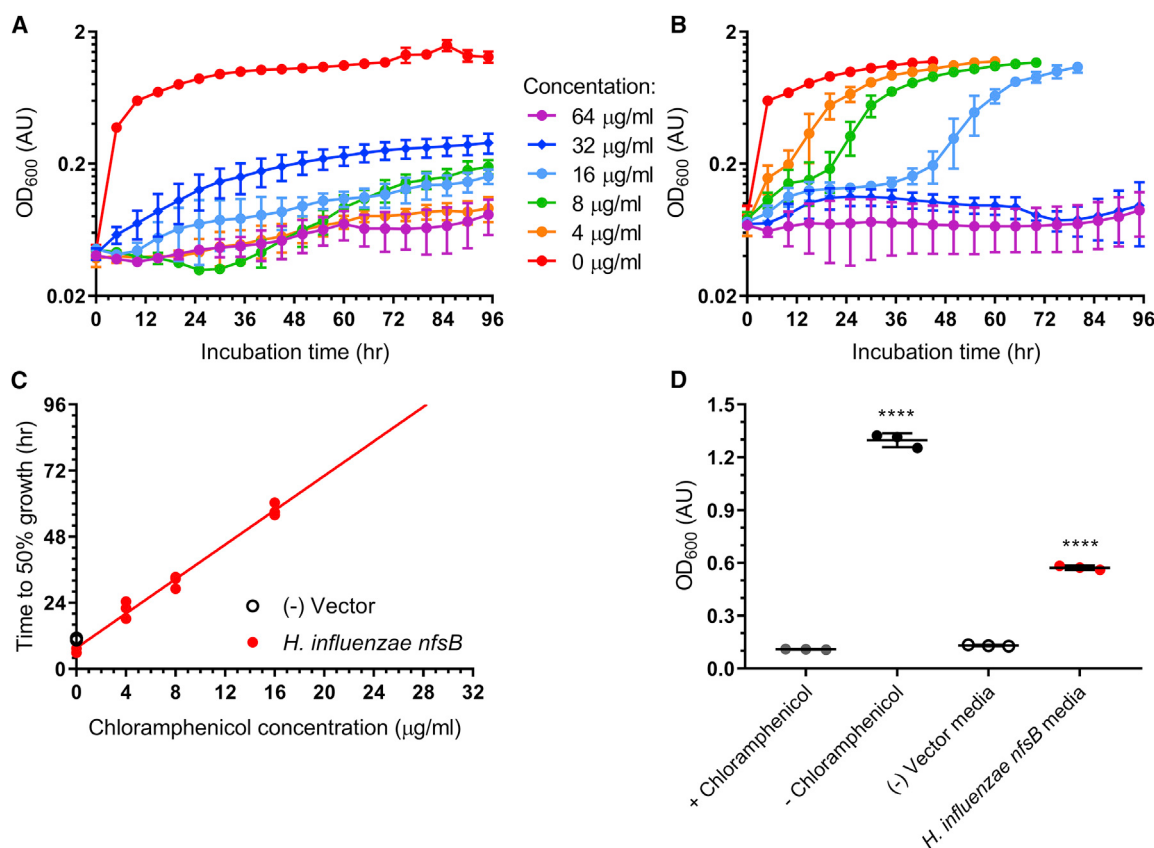


Figure 4. Chloramphenicol Resistance in *E. coli* Expressing *H. influenzae nfsB* Occurs via a Drug-Modification Mechanism

(A and B) Lag-phase assays of *E. coli* expressing (A) empty vector or (B) *H. influenzae nfsB* grown in the presence of increasing concentrations of chloramphenicol ranging from 0 µg/mL to 64 µg/mL.

(C) Linear regression of incubation time required to reach half-maximal OD₆₀₀ plotted against chloramphenicol concentration. The slope of the fit line is 3.12 ± 0.11 with an R² of 0.998.

(D) Growth of chloramphenicol-susceptible *E. coli* in chloramphenicol medium pre-conditioned by empty vector or reductase-expressing *E. coli* strains. All experiments were performed in triplicate with error bars representing SD when present. Significance at ***p ≤ 0.0001 was calculated based on triplicate experiments using a one-way ANOVA test with Dunnett's correction for multiple comparisons, and reflects a comparison with vector control.

enzymatic activity by following chloramphenicol degradation over the course of time. Two reactions were initiated by adding enzyme or buffer to solutions containing chloramphenicol and NADPH, following which paired aliquots were quenched every 2.5 min for quantitative analysis of chloramphenicol concentrations. LC-MS analysis confirmed loss of chloramphenicol in the enzyme reactions but not in the control reaction (Figures 5A and 5B).

For confirmation that the product of this reaction was amino-chloramphenicol, a preparative scale reaction with an NADPH regeneration system was incubated for 22.5 hr, extracted with ethyl acetate, and the resulting products analyzed by LC-MS. Extraction of ion m/z corresponding to amino-chloramphenicol revealed peaks at the same retention time as standards (Figures 5C and S3A), with the first peak exhibiting a mass spectrum and retention time consistent with amino-chloramphenicol (Figure 5D). Verification of amino-chloramphenicol as a product of *H. influenzae* NfsB reduction of chloramphenicol was completed by comparison of product with standard by multiple-reaction monitoring (MRM) mass spectrometry fragment analysis (Figures S3B and S3C).

Nitrated Compounds and Chloramphenicol, but Not Other Amphenicols, Are *H. influenzae* NfsB Substrates

Nitroreductase enzymes generally show wide substrate specificity (Akiva et al., 2017; Pitsawong et al., 2014; Roldán et al., 2008), so we next set out to more thoroughly characterize the substrate range of the *H. influenzae* NfsB enzyme and its kinetics. We first attempted to measure crude chloramphenicol reduction kinetics via the Bratton-Marshall derivatization test (Bratton and Marshall, 1939), using time-quenched reaction samples as inputs. The Bratton-Marshall assay is sensitive and specific for aromatic amines but not other aromatic nitrogenous substituents, and is especially apt for detecting amino-chloramphenicol (Bratton and Marshall, 1939; Glazko, 1987b; Smith et al., 2007). Reaction progress curves of Bratton-Marshall-positive products at different concentrations of chloramphenicol indicated enzymatic production of amino-chloramphenicol and suggested that the *H. influenzae* NfsB enzyme follows Michaelis-Menten kinetics (Figure S4A). Nitroreductase reactions can be followed in real time spectrophotometrically by measuring the oxidation of NAD(P)H to NAD(P) (Mermod et al., 2010). To confirm that *H. influenzae* NfsB oxidation of NADPH

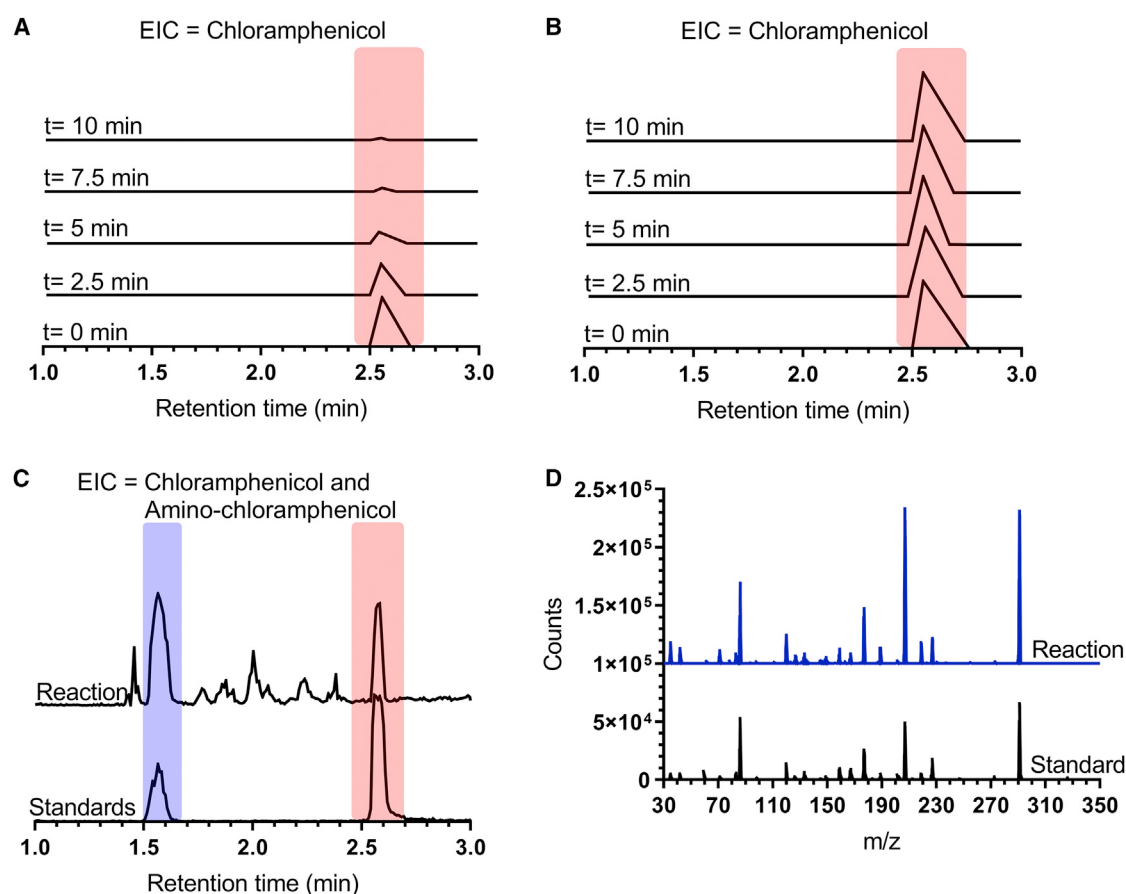


Figure 5. Analytical Characterization of *H. influenzae* NfsB Chloramphenicol Reduction Products

(A and B) LC-MS monitoring of loss of chloramphenicol (323.132 m/z , monitored at 321 m/z) over 10 min in the presence (A) and absence (B) of enzyme. (C and D) LC-MS analysis of products extracted from overnight enzymatic reaction with chloramphenicol and NADPH regeneration system. (C) Extracted ion counts corresponding to amino-chloramphenicol (291 m/z , blue bar) and chloramphenicol (321 m/z , red bar) of reaction products (top traces) compared with co-mixed amino-chloramphenicol and chloramphenicol standards (bottom traces). (D) Mass spectra of 1.6-min retention time product peak (blue trace) compared with amino-chloramphenicol standard (black trace).

corresponds to chloramphenicol reduction, we followed the same reaction wells at a wavelength specific to NADPH (beyond the absorbance range of chloramphenicol, Figure S4B) and at a wavelength specific to the chloramphenicol nitro group (at the isosbestic point of NADPH/NADP), as determined by comparison of UV-visible spectra of chloramphenicol and the nitro group free amphenicols thiamphenicol and florfenicol (Figure S4B). The resulting progress curves (Figures S4C and S4D) match closely, confirming NADPH monitoring as an appropriate proxy for nitroreduction.

We next measured the kinetics of *H. influenzae* NfsB reduction of chloramphenicol, as well as other potential aromatic nitro-substrates. We began by comparing reduction of chloramphenicol with reduction of thiamphenicol and florfenicol. Because thiamphenicol and florfenicol do not contain nitro groups, we expected to see no activity with these substrates. Of the three amphenicols, only the reaction containing chloramphenicol showed evidence of enzymatic activity, demonstrating classic Michaelis-Menten kinetics (Figure 6A). NfsB and other nitroreductase enzymes are the targets of the 5-nitro class of antibiotics,

including metronidazole and nitrofurantoin. These antibiotics are pro-drugs and become bactericidal when reductases act on their aromatic nitrogen groups, leading to the production of highly reactive hydroxylamines (Dingsdag and Hunter, 2018). We assayed the activity of *H. influenzae* NfsB against these two compounds and confirmed that both are substrates, with nitrofurantoin in particular showing rapid turnover rates (Figure 6B). Finally, we also assayed 3- and 4-nitrophenol as well as menadione, a quinone lacking nitro groups that is often nonetheless reduced by NfsB nitroreductases (Zenno et al., 1996b). All three of these compounds also acted as substrates, with menadione showing relatively high activity and 4-nitrophenol showing relatively low activity (Figure 6C). Michaelis-Menten kinetics for each substrate are reported in Table S2.

Subsequently, we performed Bratton-Marshall endpoint assays on reactions with each nitro-containing substrate (substrates listed above except thiamphenicol, florfenicol, and menadione), as well as enzyme and cofactor controls. As expected, the control lacking NADPH showed very little production of Bratton-Marshall-derivatized material, while the full

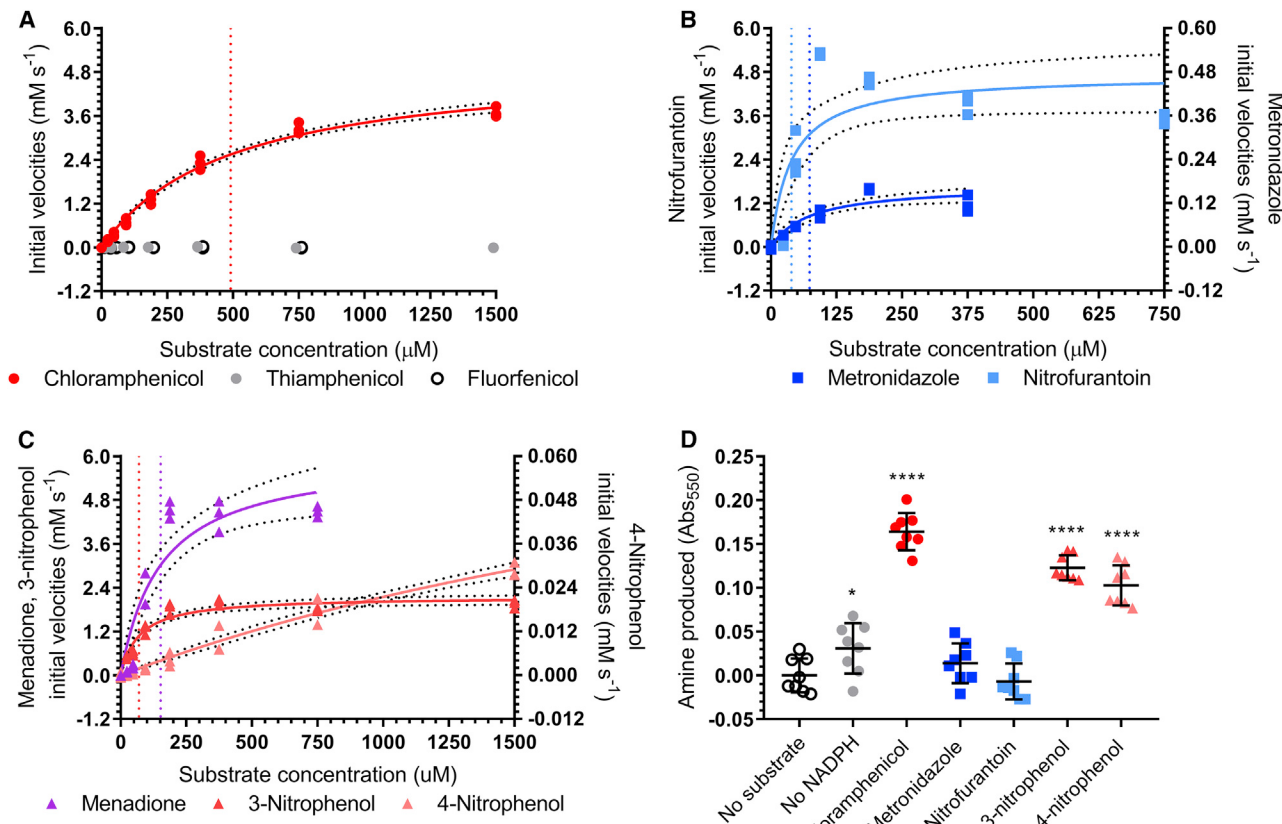


Figure 6. *H. influenzae* NfsB Shows Michaelis-Menten Kinetics with Chloramphenicol, Menadione, and Nitro-Substrates

(A–C) Graphs of Michaelis-Menten kinetics for *H. influenzae* NfsB with k_{cat}/K_M ($\text{mM}^{-1} \text{s}^{-1}$) for the following substrate groups (nd, not determined): (A) amphenicols (chloramphenicol 20.71, thiamphenicol nd, and florfenicol nd), (B) 5-nitro antibiotics (metronidazole 4.57 and nitrofurantoin 242.89), and (C) other substrates (menadione 79.34, 3-nitrophenol 61.80, and 4-nitrophenol nd). All reactions were performed in triplicate and the best-fit Michaelis-Menten kinetics curves (solid lines) and corresponding 95% confidence intervals (dotted lines) are shown. Vertical dotted lines correspond to the calculated K_M values and are color coded by substrate within each panel. In (A), florfenicol and thiamphenicol points are offset for clarity.

(D) Bratton-Marshall analysis of aryl amine formation in reactions containing *H. influenzae* NfsB. Reactions contained enzyme, FMN, NADPH, and substrate unless otherwise noted. Reactions were performed in eight technical replicates with mean and SD shown. Significance compared with no substrate (at ****p ≤ 0.0001 and *p ≤ 0.05) was calculated using a one-way ANOVA test with Dunnett's correction for multiple comparisons.

chloramphenicol reaction showed a significant amount. In contrast, the 5-nitro antibiotics showed no significant production compared with the substrate control reaction, while the two nitrophenol compounds showed intermediate levels (Figure 6D).

Metronidazole Inhibits Chloramphenicol Reduction by *H. influenzae* NfsB In Vitro and Synergizes with Chloramphenicol to Inhibit *E. coli* Expressing nfsB

During the course of our *in vitro* experiments we were surprised to see that the *H. influenzae* NfsB enzyme reduces chloramphenicol to amino-chloramphenicol (Figures 5 and S3) and also uses metronidazole as a substrate (Figure 6C), but does not reduce the metronidazole nitro group all the way to an amino group (Figure 6D). Because partial reduction of the aromatic nitro group underlies the bactericidal activity of 5-nitro class of antibiotics such as metronidazole (Dingsdag and Hunter, 2018), we next assayed *E. coli* expressing *nfsB* homologs from *H. influenzae* and *E. cloacae*, as well as from *S. enterica* and *E. coli*, for altered susceptibility to metronidazole. Metronidazole susceptibility is

usually limited to anaerobic bacteria (Dingsdag and Hunter, 2018), as illustrated by the high IC₅₀ ($23.7 \pm 2.0 \mu\text{g/mL}$) of our vector control. All four *E. coli* strains expressing *nfsB* homologs showed significantly increased susceptibility to metronidazole compared with the vector control, with the strains expressing the *H. influenzae* and *E. cloacae* *nfsB* genes showing the most sensitivity (Figures S5A and S5B).

Based on the antibiotic susceptibility evidence, *H. influenzae* *nfsB* expression is advantageous in the presence of chloramphenicol, providing resistance through reduction (Figure 2). However, in the presence of metronidazole *nfsB* expression is disadvantageous, as *E. coli* does not normally activate metronidazole to its toxic form but appears to do so under these conditions (Figures S5A and S5B). Our kinetics data (Table S2) also suggest that, based on K_M measures, metronidazole should be able to compete with chloramphenicol substrate binding. We therefore hypothesized that chloramphenicol and metronidazole might act synergistically when used in combination against chloramphenicol-reducing bacteria. We found that by increasing

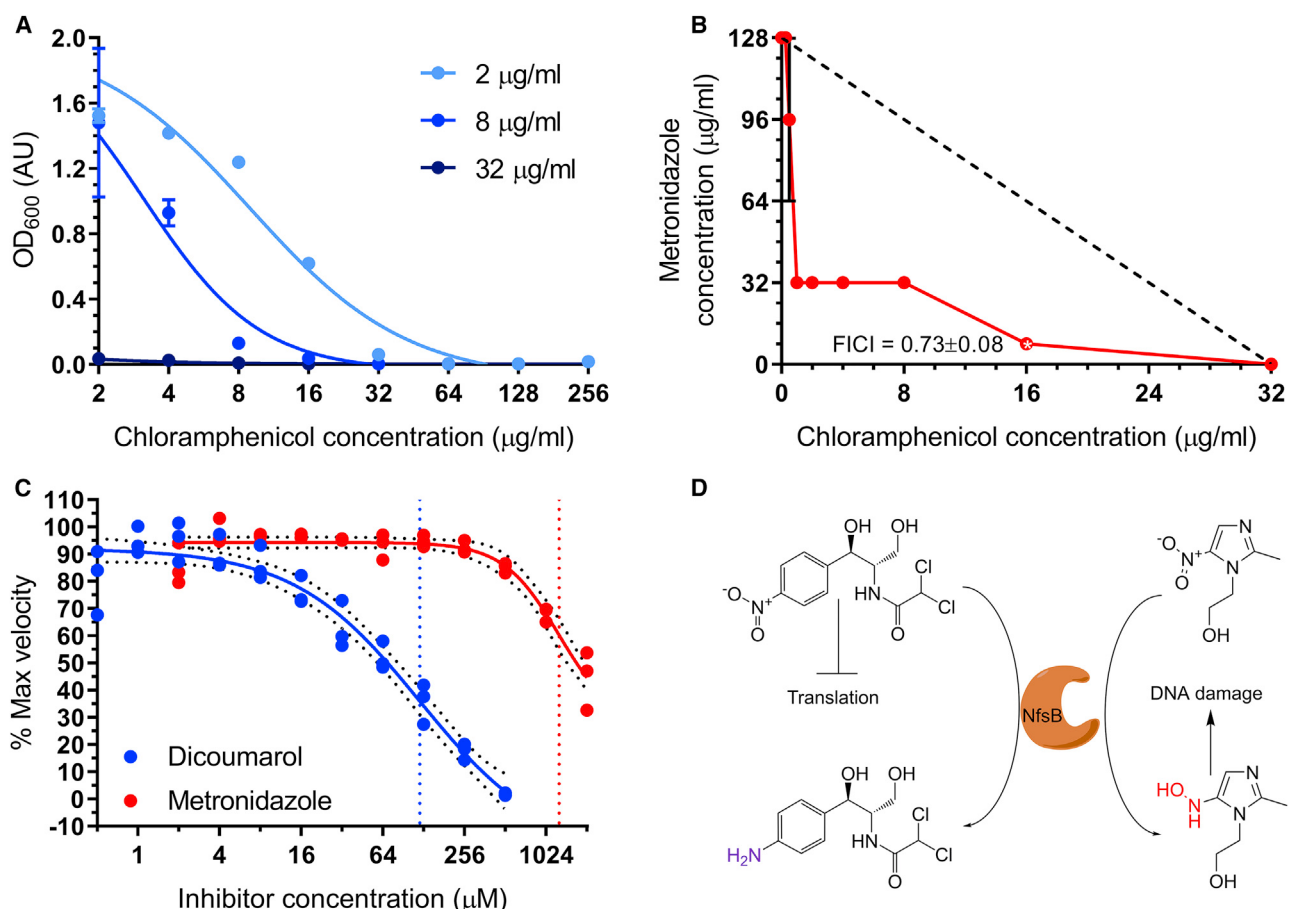


Figure 7. Inhibition of Chloramphenicol Reduction and Synergistic Killing by Metronidazole

(A) Dose-response curves of *E. coli* expressing *H. influenzae nfsB* at various concentrations of chloramphenicol and the indicated concentrations of metronidazole (2 $\mu\text{g/mL}$, 8 $\mu\text{g/mL}$, and 32 $\mu\text{g/mL}$).

(B) FICI analysis of metronidazole versus chloramphenicol 2D checkerboard assay. The lowest FICI score of 0.73 ± 0.08 was found at 16 $\mu\text{g/mL}$ chloramphenicol and 8 $\mu\text{g/mL}$ metronidazole. Dashed black line represents theoretical line of additivity. (A) and (B) report mean of three replicate experiments with SD error bars.

(C) *In vitro* assay of chloramphenicol reduction inhibition by dicoumarol (blue curve) or metronidazole (red curve). 95% confidence intervals of curve fits of triplicate data points are shown (black dotted lines), and fit IC₅₀ (vertical colored lines) are indicated (dicoumarol 119.7 μM ; metronidazole 1,274 μM).

(D) Schematic representation of the role of NfsB in synergy experiment: (left) chloramphenicol resistance and (right) metronidazole toxic activation, both via nitroreduction.

the concentration of metronidazole, the chloramphenicol susceptibility of the *H. influenzae nfsB* expression *E. coli* strain increased markedly (Figure 7A).

Our follow-up analysis using a checkerboard-type assay to measure interactions between the antibiotics demonstrated that chloramphenicol and metronidazole do indeed act synergistically in *E. coli* expressing *H. influenzae nfsB*, with the lowest fractional inhibitory concentration indices (FICI) score reaching 0.727 ± 0.080 (Figure 7B), significantly lower than *E. coli* with empty vector (FICI = 2.30 ± 0.73). We further studied this interaction *in vitro* by measuring the rate of chloramphenicol reduction in the presence of increasing concentrations of metronidazole or dicoumarol, a known inhibitor of NfsB enzymes (Roldán et al., 2008). *In vitro* we observed that both substrates have the potential to inhibit chloramphenicol reduction, though with metronidazole showing an IC₅₀ of ~1 mM (Figure 7C). The hypothesized interplay between resistance via reduction and pro-drug activation via reduction is summarized in Figure 7D.

DISCUSSION

We present results from a series of cross-validating experiments that demonstrate the ability of *H. influenzae* NfsB to reduce the nitro group of chloramphenicol. We provide the identification and characterization of an enzyme with chloramphenicol reductase activity, beginning with its ability to confer resistance to chloramphenicol when expressed in *E. coli* (Figure 2). While resistance was not as thorough as that seen in *E. coli* expressing the *cat* gene, resistance conferred by *H. influenzae nfsB* allowed for growth well beyond the EUCAST clinical breakpoint for *E. coli* of 8 $\mu\text{g/mL}$. Similarly, expression of the *nfsB* homolog from *E. cloacae* was sufficient to confer increased resistance to chloramphenicol in *E. coli*, again above the clinical breakpoint for defining resistance.

We were curious as to whether we could detect a signal in the amino acid sequence of the *H. influenzae* NfsB enzyme that could predict its heightened ability to resist chloramphenicol

but were unable to do so (Figure 3), suggesting that structural studies may be warranted. Nevertheless, the phylogenetic distance between *H. influenzae* and *E. cloacae* NfsB proteins suggests to us that chloramphenicol reduction may be relatively widely spread. Chloramphenicol is a natural product antibiotic that has been recovered from across the globe (Ehrlich et al., 1947; Gottlieb and Bhattacharya, 1948) and is detectable in the soil at low concentrations (Berendsen et al., 2013), suggesting that nitroreduction may be a feasible resistance mechanism against environmental levels of the drug.

We also found compelling evidence for utility of this resistance mechanism in the face of clinical therapy. In addition to growing in the presence of chloramphenicol concentrations above resistance breakpoints (Figure 2), we found in a different assay that *E. coli* expressing *H. influenzae nfsB* appears capable of detoxifying increasing levels of chloramphenicol given enough time (Figure 4). This finding is in agreement with a literature report (Onderdonk et al., 1979) that during infection, *Bacteroides fragilis* strains that showed *in vitro* susceptibility to chloramphenicol were capable of resisting treatment through reduction. It is also possible, therefore, that during treatment with chloramphenicol commensal or pathogenic bacteria may find a selective advantage in reducing the nitro group of chloramphenicol.

In vitro, the *H. influenzae* NfsB enzyme is capable of reducing the chloramphenicol nitro group completely to an amine, as well as potentially the nitro groups of other nitrophenols (Figures 5 and 6). Complete reduction of aromatic nitro groups is a rare feature among described NfsB homologs (Pitsawong et al., 2014; Roldán et al., 2008) that may have further industrial or medical applications (Copp et al., 2017). The kinetics of chloramphenicol reduction (Table S2), with a k_{cat}/K_M of $20.71 \text{ mM}^{-1} \text{ s}^{-1}$, are slower than many canonical antibiotic resistance enzymes, such as diffusion-limited β -lactamases, but fall within the range of kinetics observed for average enzymes (Bar-Even et al., 2011). The NfsB enzyme from *H. influenzae* appears to have promiscuous substrate binding, based on the variety of substrates it is capable of turning over and their K_M s, ranging from roughly $40 \mu\text{M}$ to $500 \mu\text{M}$. In this respect it is similar to other nitroreductase enzymes which, as a class, show substrate promiscuity and relatively weak substrate binding (Akiva et al., 2017; Bryant and DeLuca, 1991; Pitsawong et al., 2014; Race et al., 2005; Roldán et al., 2008). Of the substrates tested, *H. influenzae* NfsB showed the greatest activity with nitrofurantoin and lowest reliably measured activity with metronidazole, with k_{cat}/K_M measures approximately an order of magnitude above and below that measured for chloramphenicol, respectively. Despite their wide difference in kinetics, reactions containing neither nitrofurantoin nor metronidazole showed evidence for the production of aromatic amino groups (Figure 6D). Partial reduction of these compounds is the key to their antibiotic activity, but full reduction can provide resistance (Roldán et al., 2008). In the case of *H. influenzae* NfsB, reduction is sufficient to provide resistance to chloramphenicol, but might only serve to more fully activate the antibacterial activity of metronidazole and nitrofurantoin.

In exploring this idea further, we found that expression of *H. influenzae nfsB* and other *nfsB* homologs in *E. coli* leads to significantly increased susceptibility to metronidazole, a drug that is usually only used to treat anaerobes (Figures S5A and S5B). We further observed that metronidazole potentiates chlor-

amphenicol resistance in the *H. influenzae nfsB*-expressing strain and that in fact the two antibiotics synergistically inhibit the growth of this strain (Figures 7A and 7B). We hypothesized that this synergy may be the result of two activities. The first of these relates to our observation that metronidazole is not fully reduced to form an amino group, but does act as an NfsB substrate. Therefore it is likely that while NfsB protects the cell against chloramphenicol it also activates metronidazole to its lethal form, counteracting any survival benefit. The second activity that we believe might be relevant is substrate inhibition. While metronidazole is a poor substrate compared with chloramphenicol as measured by k_{cat} (0.337 s^{-1} versus 10.17 s^{-1}) it is much better when measured by K_M ($74 \mu\text{M}$ versus $\sim 500 \mu\text{M}$) (Table S2). We hypothesized that metronidazole may therefore be able to compete with chloramphenicol as a substrate, a hypothesis borne out by our measurements of chloramphenicol reduction in the presence of titrated metronidazole (Figure 7C). A schematic of chloramphenicol/metronidazole synergy is presented in Figure 7D, wherein metronidazole directly kills *H. influenzae*-expressing *E. coli* via its reduction-mediated activation to a toxic form and indirectly inhibits growth of this strain by competing with chloramphenicol, resulting in diminished resistance to it.

Finally, it has been hypothesized that chloramphenicol nitroreduction by host-associated bacteria underlies the development of a rare, serious side effect of chloramphenicol, namely aplastic anemia (Holt, 1967). The lack of mechanistic understanding of chloramphenicol-induced aplastic anemia is largely responsible for the failure of many developed countries to utilize amphenicols in the clinic, including potentially superior second- and third-generation compounds. For example, florfénicol, which lacks a nitro group, is immune to inactivation by chloramphenicol acetyl-transferases (Dinos et al., 2016) (Figures S5C and S5D) but is not used clinically due to fears that its use in humans may result in development of aplastic anemia. The identification of a bacterial enzyme capable of chloramphenicol reduction provides the prerequisite for testing the aplastic anemia hypothesis and potentially shedding light on the safety of nitro group free amphenicols.

SIGNIFICANCE

Chloramphenicol was first identified as a potent antibiotic more than 70 years ago, and since then a number of bacterial resistance mechanisms against it have been identified. However, the enzyme underlying the first reported mechanism of chloramphenicol resistance, reduction of the nitro group to an amine, has remained elusive despite numerous reports of bacteria showing this activity. We describe an example of an enzyme with this activity, the oxygen-insensitive nitroreductase NfsB from *Haemophilus influenzae*. Expression of the gene for this enzyme, or its homolog from *Enterobacter cloacae*, is sufficient to confer resistance to chloramphenicol in *Escherichia coli*. In vitro characterization of the purified enzyme revealed its ability to fully reduce aromatic nitro groups on a variety of substrates and partially reduce the nitro groups of metronidazole and nitrofurantoin, two antibiotics that gain their ability to kill bacteria following reduction. We found that expression of the *H. influenzae* nitroreductase gene in *E. coli* augments the killing power of metronidazole and potentiates the efficacy of chloramphenicol, likely

through both direct and indirect mechanisms. Finally, identification of this enzyme closes a long-open chapter in chloramphenicol resistance and potentially provides a clue to the mechanistic basis of one of chloramphenicol's serious side effects, aplastic anemia, that has prevented adoption of promising chloramphenicol analogs in the clinic.

STAR★METHODS

Detailed methods are provided in the online version of this paper and include the following:

- **KEY RESOURCES TABLE**
- **CONTACT FOR REAGENT AND RESOURCE SHARING**
- **EXPERIMENTAL MODEL AND SUBJECT DETAILS**
- **METHODS DETAILS**
 - Gene Amplification and Cloning
 - Microbroth Serial Dilution Assays
 - Phylogenetic Analysis of Reductase Proteins
 - Lag-Phase Chloramphenicol Modification Assay
 - Pre-conditioned Media Assay
 - *H. influenzae* NfsB Expression and Purification
 - Chloramphenicol Reduction Assay Optimization
 - Chloramphenicol Modification LCMS Assay
 - Amino-Chloramphenicol Detection Assay
 - Enzyme Substrate Specificity and Activity
 - Checkerboard Assay to Detect Synergy
 - *In Vitro* Inhibition of Chloramphenicol Reduction
- **QUANTIFICATION AND STATISTICAL ANALYSIS**

SUPPLEMENTAL INFORMATION

Supplemental Information includes five figures and two tables and can be found with this article online at <https://doi.org/10.1016/j.chembiol.2019.01.007>.

ACKNOWLEDGMENTS

Support for this work came in part by awards to G.D. through the Edward Mallinckrodt, Jr. Foundation (Scholar Award), the NIH Director's New Innovator Award (<http://commonfund.nih.gov/newinnovator/>), the National Institute of Diabetes and Digestive and Kidney Diseases (NIDDK: <http://www.niddk.nih.gov/>), the National Institute of General Medical Sciences (NIGMS: <http://www.nigms.nih.gov/>), and the National Institute of Allergy and Infectious Diseases (NIAID: <https://www.niaid.nih.gov/>) of the National Institutes of Health (NIH) under award numbers DP2DK098089, R01GM099538, and R01AI123394, respectively. T.S.C. was supported by the <http://www2.niddk.nih.gov/> National Institute of Diabetes and Digestive and Kidney Diseases training grant through award number T32 DK077653 (Phillip I. Tarr, Principal Investigator) and the National Institute of Child Health and Development training grant through award number T32 HD049305 (Kelle H. Moley, Principal Investigator). Mass spectrometry was performed in the Metabolomics Facility at Washington University (P30 DK020579). The content is solely the responsibility of the authors and does not necessarily represent the official views of the funding agencies. We are thankful to the Caparon lab for supplying *S. pyogenes* genomic DNA, to Dr. Tim Wencewicz for his insightful discussions regarding enzymology and biochemistry, and to Drew Gasparrini and the rest of the Dantas lab for many helpful discussions of the work and manuscript.

AUTHOR CONTRIBUTIONS

Conceptualization, T.S.C. and G.D.; Methodology, T.S.C. and G.D.; Investigation, T.S.C., P.S., A.O.K., B.W., B.A.B., N.Z., and J.G.; Writing – Original Draft, T.S.C.; Writing – Review & Editing, T.S.C., P.S., and G.D.; Supervision, T.S.C.

and G.D. Mass spectrometry was performed in the Metabolomics Facility at Washington University.

DECLARATION OF INTERESTS

The authors declare no competing interests.

Received: August 1, 2018

Revised: November 6, 2018

Accepted: January 14, 2019

Published: February 21, 2019

REFERENCES

- Avika, E., Copp, J.N., Tokuriki, N., and Babbitt, P.C. (2017). Evolutionary and molecular foundations of multiple contemporary functions of the nitroreductase superfamily. *Proc. Natl. Acad. Sci. U S A* **114**, E9549–E9558.
- Bar-Even, A., Noor, E., Savir, Y., Liebermeister, W., Davidi, D., Tawfik, D.S., and Milo, R. (2011). The moderately efficient enzyme: evolutionary and physicochemical trends shaping enzyme parameters. *Biochemistry* **50**, 4402–4410.
- Berendsen, B., Pikkemaat, M., Römkens, P., Wegh, R., van Sisseren, M., Stolk, L., and Nielen, M. (2013). Occurrence of chloramphenicol in crops through natural production by bacteria in soil. *J. Agric. Food Chem.* **61**, 4004–4010.
- Bratton, A., and Marshall, E.K., Jr. (1939). A new coupling component for sulfanilamide determination. *J. Biol. Chem.* **128**, 537–550.
- Bryant, C., and DeLuca, M. (1991). Purification and characterization of an oxygen-insensitive NAD(P)H nitroreductase from *Enterobacter cloacae*. *J. Biol. Chem.* **266**, 4119–4125.
- Čivljak, R., Giannella, M., Di Bella, S., and Petrosillo, N. (2014). Could chloramphenicol be used against ESKAPE pathogens? A review of in vitro data in the literature from the 21st century. *Expert Rev. Anti. Infect. Ther.* **12**, 249–264.
- Copp, J.N., Mowday, A.M., Williams, E.M., Guise, C.P., Ashoorzadeh, A., Sharrock, A.V., Flanagan, J.U., Smail, J.B., Patterson, A.V., and Ackery, D.F. (2017). Engineering a multifunctional nitroreductase for improved activation of prodrugs and PET probes for cancer gene therapy. *Cell Chem. Biol.* **24**, 391–403.
- Crofts, T.S., Gasparrini, A.J., and Dantas, G. (2017). Next-generation approaches to understand and combat the antibiotic resistome. *Nat. Rev. Microbiol.* **15**, 422–434.
- Crofts, T.S., Wang, B., Spivak, A., Gianoulis, T.A., Forsberg, K.J., Gibson, M.K., Johnsky, L.A., Broomall, S.M., Rosenzweig, C.N., Skowronski, E.W., et al. (2018). Shared strategies for β-lactam catabolism in the soil microbiome. *Nat. Chem. Biol.* **14**, 556–564.
- Dingsdag, S.A., and Hunter, N. (2018). Metronidazole: an update on metabolism, structure-cytotoxicity and resistance mechanisms. *J. Antimicrob. Chemother.* **73**, 265–279.
- Dinos, G., Athanassopoulos, C., Missiri, D., Giannopoulou, P., Vlachogiannis, I., Papadopoulos, G., Papaioannou, D., and Kalpaxis, D. (2016). Chloramphenicol derivatives as antibacterial and anticancer agents: historic problems and current solutions. *Antibiotics (Basel)* **5**, 20.
- Egami, F., Ebata, M., and Sato, R. (1951). Reduction of chloromycetin by a cell-free bacterial extract and its relation to nitrite reduction. *Nature* **167**, 118–119.
- Ehrlich, J., Bartz, Q.R., Smith, R.M., Joslyn, D.A., and Burkholder, P.R. (1947). Chloromycetin, a new antibiotic from a soil actinomycete. *Science* **106**, 417.
- Eliakim-Raz, N., Lador, A., Leibovici-Weissman, Y., Elbaz, M., Paul, M., and Leibovici, L. (2015). Efficacy and safety of chloramphenicol: joining the revival of old antibiotics? Systematic review and meta-analysis of randomized controlled trials. *J. Antimicrob. Chemother.* **70**, 979–996.
- Gasteiger, E., Gattiker, A., Hoogland, C., Ivanyi, I., Appel, R.D., and Bairoch, A. (2003). ExPASy: the proteomics server for in-depth protein knowledge and analysis. *Nucleic Acids Res.* **31**, 3784–3788.
- Glazko, A.J. (1987a). Early adventures in drug metabolism. 3. Chloramphenicol. *Ther. Drug Monit.* **9**, 320–330.

- Glazko, A.J. (1987b). Early adventures in drug metabolism: 1. Role of the Bratton-Marshall reagent. *Ther. Drug Monit.* 9, 53–60.
- Glazko, A.J., Dill, W.A., and Wolf, L.M. (1952). Observations on the metabolic disposition of chloramphenicol (chloromycetin) in the rat. *J. Pharmacol. Exp. Ther.* 104, 452–458.
- Gottlieb, D., and Bhattacharya, P.K. (1948). Some properties of an antibiotic obtained from a species of *Streptomyces*. *J. Bacteriol.* 55, 409–417.
- Holt, R. (1967). The bacterial degradation of chloramphenicol. *Lancet* 1, 1259–1260.
- Holt, D.E., Hurley, R., and Harvey, D. (1995). A reappraisal of chloramphenicol metabolism: detection and quantification of metabolites in the sera of children. *J. Antimicrob. Chemother.* 35, 115–127.
- Kinch, M.S., Patridge, E., Plummer, M., and Hoyer, D. (2014). An analysis of FDA-approved drugs for infectious disease: antibacterial agents. *Drug Discov. Today* 19, 1283–1287.
- Kumar, S., Stecher, G., and Tamura, K. (2016). MEGA7: molecular evolutionary genetics analysis version 7.0 for bigger datasets. *Mol. Biol. Evol.* 33, 1870–1874.
- Kunin, C.M., Glazko, A.J., and Finland, M. (1959). Persistence of antibiotics in blood of patients with acute renal failure. II. Chloramphenicol and its metabolic products in the blood of patients with severe renal disease or hepatic cirrhosis. *J. Clin. Invest.* 38, 1498–1508.
- Li, J., Nation, R.L., Turnidge, J.D., Milne, R.W., Coulthard, K., Rayner, C.R., and Paterson, D.L. (2006). Colistin: the re-emerging antibiotic for multidrug-resistant Gram-negative bacterial infections. *Lancet Infect. Dis.* 6, 589–601.
- Lim, C., Takahashi, E., Hongsuwan, M., Wuthiekanun, V., Thamlikitkul, V., Hinjoy, S., Day, N.P., Peacock, S.J., and Limmathurotsakul, D. (2016). Epidemiology and burden of multidrug-resistant bacterial infection in a developing country. *Elife* 5, e18082.
- LinWu, S.W., Syu, C.J., Chen, Y.L., Wang, A.H.J., and Peng, F.C. (2009). Characterization of *Escherichia coli* nitroreductase NfsB in the metabolism of nitrobenzodiazepines. *Biochem. Pharmacol.* 78, 96–103.
- Long, K.S., Poehlsgaard, J., Kehrenberg, C., Schwarz, S., and Vester, B. (2006). The Cfr rRNA methyltransferase confers resistance to phenolics, lincosamides, oxazolidinones, pleuromutilins, and streptogramin A antibiotics. *Antimicrob. Agents Chemother.* 50, 2500–2505.
- Lutz, R., and Bujard, H. (1997). Independent and tight regulation of transcriptional units in *Escherichia coli* via the LacR/O, the TetR/O and AraC/I1-I2 regulatory elements. *Nucleic Acids Res.* 25, 1203–1210.
- Merkel, J.R., and Steers, E. (1953). Relationship between chloramphenicol reductase activity and chloramphenicol resistance in *Escherichia coli*. *J. Bacteriol.* 66, 389–396.
- Mermod, M., Mourlanc, F., Waltersperger, S., Oberholzer, A.E., Baumann, U., and Solioz, M. (2010). Structure and function of CinD (YtiD) of *Lactococcus lactis*, a copper-induced nitroreductase involved in defense against oxidative stress. *J. Bacteriol.* 192, 4172–4180.
- Nitzan, O., Suponitzky, U., Kennes, Y., Chazan, B., Raz, R., and Colodner, R. (2010). Is chloramphenicol making a comeback? *Isr. Med. Assoc. J.* 12, 371–374.
- O'Brien, R.W., and Morris, J.G. (1971). The ferredoxin-dependent reduction of chloramphenicol by *Clostridium acetobutylicum*. *J. Gen. Microbiol.* 67, 265–271.
- O'Neil, J. (2014). The Review on Antimicrobial Resistance (Wellcome Trust and UK Department of Health). <https://amr-review.org/>.
- Onderdonk, A.B., Kasper, D.L., Mansheim, B.J., Louie, T.J., Gorbach, S.L., and Bartlett, J.G. (1979). Experimental animal models for anaerobic infections. *Rev. Infect. Dis.* 1, 291–301.
- Payne, D.J., Gwynn, M.N., Holmes, D.J., and Pompliano, D.L. (2007). Drugs for bad bugs: confronting the challenges of antibacterial discovery. *Nat. Rev. Drug Discov.* 6, 29–40.
- Pitsawong, W., Hoben, J.P., and Miller, A.F. (2014). Understanding the broad substrate repertoire of nitroreductase based on its kinetic mechanism. *J. Biol. Chem.* 289, 15203–15214.
- Pye, C.R., Bertin, M.J., Lokey, R.S., Gerwick, W.H., and Linington, R.G. (2017). Retrospective analysis of natural products provides insights for future discovery trends. *Proc. Natl. Acad. Sci. U S A* 114, 5601–5606.
- Race, P.R., Lovering, A.L., Green, R.M., Ossor, A., White, S.A., Searle, P.F., Wrighton, C.J., and Hyde, E.I. (2005). Structural and mechanistic studies of *Escherichia coli* nitroreductase with the antibiotic nitrofurazone. Reversed binding orientations in different redox states of the enzyme. *J. Biol. Chem.* 280, 13256–13264.
- Rahim, N.A., Cheah, S.E., Johnson, M.D., Yu, H., Sidjabat, H.E., Boyce, J., Butler, M.S., Cooper, M.A., Fu, J., Paterson, D.L., et al. (2015). Synergistic killing of NDM-producing *MDR Klebsiella pneumoniae* by two “old” antibiotics-polymyxin B and chloramphenicol. *J. Antimicrob. Chemother.* 70, 2589–2597.
- Rambaut, A. (2008). FigTree v1.1.1: Tree Figure Drawing Tool. <https://github.com/rambaut/figtree/releases>.
- Roldán, M.D., Pérez-Reinado, E., Castillo, F., and Moreno-Vivián, C. (2008). Reduction of polynitroaromatic compounds: the bacterial nitroreductases. *FEMS Microbiol. Rev.* 32, 474–500.
- Schwarz, S., Kehrenberg, C., Doublet, B., and Cloeckaert, A. (2004). Molecular basis of bacterial resistance to chloramphenicol and florfenicol. *FEMS Microbiol. Rev.* 28, 519–542.
- Shu, X.O., Gao, Y.T., Linet, M.S., Brinton, L.A., Gao, R.N., Jin, F., and Fraumeni, J.F. (1987). Chloramphenicol use and childhood leukaemia in Shanghai. *Lancet* 2, 934–937.
- Smith, G.N., and Worrel, C.S. (1949). Enzymatic reduction of chloramphenicol. *Arch. Biochem.* 24, 216–223.
- Smith, G.N., and Worrel, C.S. (1950). The decomposition of chloromycetin (chloramphenicol) by microorganisms. *Arch. Biochem.* 28, 232–241.
- Smith, G.N., and Worrel, C.S. (1953). Reduction of chloromycetin and related compounds by *Escherichia coli*. *J. Bacteriol.* 65, 313–317.
- Smith, A.L., Erwin, A.L., Kline, T., Unrath, W.C.T., Nelson, K., Weber, A., and Howald, W.N. (2007). Chloramphenicol is a substrate for a novel nitroreductase pathway in *Haemophilus influenzae*. *Antimicrob. Agents Chemother.* 51, 2820–2829.
- Smith, R.M., Joslyn, D.A., Gruhzit, O.M., McLean, I.W., Penner, M.A., and Ehrlich, J. (1948). Chloromycetin: biological studies. *J. Bacteriol.* 55, 425–448.
- Sood, S. (2016). Chloramphenicol—a potent armament against multi-drug resistant (MDR) gram negative bacilli? *J. Clin. Diagn. Res.* 10, DC01–DC03.
- Studier, F.W. (2005). Protein production by auto-induction in high density shaking cultures. *Protein Expr. Purif.* 41, 207–234.
- Tao, W., Lee, M.H., Wu, J., Kim, N.H., Kim, J.C., Chung, E., Hwang, E.C., and Lee, S.W. (2012). Inactivation of chloramphenicol and florfenicol by a novel chloramphenicol hydrolase. *Appl. Environ. Microbiol.* 78, 6295–6301.
- The Pew Charitable Trusts (2016). A Scientific Roadmap for Antibiotic Discovery. <https://www.pewtrusts.org/~media/assets/2016/05/ascientificroadmapforantibioticdiscovery.pdf>.
- Thompson, J.D., Higgins, D.G., and Gibson, T.J. (1994). CLUSTAL W: improving the sensitivity of progressive multiple sequence alignment through sequence weighting, position-specific gap penalties and weight matrix choice. *Nucleic Acids Res.* 22, 4673–4680.
- UniProt Consortium (2015). UniProt: a hub for protein information. *Nucleic Acids Res.* 43, D204–D212.
- Wal, J.M., Corpet, D.E., Peleran, J.C., and Bories, G.F. (1983). Comparative metabolism of chloramphenicol in germfree and conventional rats. *Antimicrob. Agents Chemother.* 24, 89–94.
- Wallerstein, R.O., Condit, P.K., Kasper, C.K., Brown, J.W., and Morrison, F.R. (1969). Statewide study of chloramphenicol therapy and fatal aplastic anemia. *JAMA* 208, 2045–2050.
- Wright, G.D. (2017). Opportunities for natural products in 21st century antibiotic discovery. *Nat. Prod. Rep.* 34, 694–701.
- Wright, P.M., Seiple, I.B., and Myers, A.G. (2014). The evolving role of chemical synthesis in antibacterial drug discovery. *Angew. Chem. Int. Ed.* 53, 8840–8869.

- Yanto, Y., Hall, M., and Bommarius, A.S. (2010). Nitroreductase from *Salmonella typhimurium*: characterization and catalytic activity. *Org. Biomol. Chem.* 8, 1826–1832.
- Zenno, S., Koike, H., Kumar, A.N., Jayaraman, R., Tanokura, M., and Saigo, K. (1996a). Biochemical characterization of NfsA, the *Escherichia coli* major nitro-reductase exhibiting a high amino acid sequence homology to Frp, a *Vibrio harveyi* flavin oxidoreductase. *J. Bacteriol.* 178, 4508–4514.
- Zenno, S., Koike, H., Tanokura, M., and Saigo, K. (1996b). Gene cloning, purification, and characterization of NfsB, a minor oxygen-insensitive nitroreductase from *Escherichia coli*, similar in biochemical properties to FRase I, the major flavin reductase in *Vibrio fischeri*. *J. Biochem.* 120, 736–744.
- Sherma, J., and Fried, B. (2003). *Handbook of Thin-Layer Chromatography* (Taylor & Francis Inc).

STAR★METHODS

KEY RESOURCES TABLE

REAGENT or RESOURCE	SOURCE	IDENTIFIER
Bacterial and Virus Strains		
<i>Escherichia coli</i> DH10B	ThermoFisher Scientific	Cat#C640003
<i>Haemophilus influenzae</i> KW20	American Type Culture Collection	ATCC#51907
<i>Salmonella enterica</i> LT2	American Type Culture Collection	ATCC#700720
<i>Enterobacter cloacae</i> 96-3	American Type Culture Collection	ATCC#13047
<i>Clostridium acetobutylicum</i> NCIB 8052	American Type Culture Collection	ATCC#824
Biological Samples		
<i>Streptococcus pyogenes</i> HSC5 genomic DNA	Caparon Laboratory	Strain HSC5
Chemicals, Peptides, and Recombinant Proteins		
NADH	Grainger	Cat#31GA86
NADPH	Cayman Chemical	Cat#9000743
NADPH regeneration system	Xenotech	Cat#K5000
Silica gel 60 TLC plates	Millipore Sigma	Cat#105794
N-2-Aminoethyl-1-naphthylamine dihydrochloride	VWR	Cat#AAA17164-09
Ammonium sulfamate	VWR	Cat#200030-422
Sodium nitrite	VWR	Cat#AA124244-14
Amino-chloramphenicol hydrochloride	Toronto Research Chemicals	Cat#A622670
Critical Commercial Assays		
Wizard Genomic DNA purification kit	Promega	Cat#A1120
Platinum Pfx polymerase	ThermoFisher Scientific	Cat#11708039
Q5 hotstart 2X master mix	New England Biosciences	Cat#M0494L
QIAquick PCR purification kit	Qiagen	Cat#28104
QIAprep Spin Miniprep kit	Qiagen	Cat#27104
Fast-Link DNA ligation kit	Epicentre	Cat#LK0750H
2X Gibson Assembly master mix	New England Biosciences	Cat#E2611S
Sypro Ruby gel stain	ThermoFisher Scientific	Cat#S12001
Bio-Safe Coomassie strain	BioRad	Cat#1610796
Ni-NTA nickel resin	BioRad	Cat#7800800
10 kDa molecular weight cut-off filter	Amicon	Cat#UFC901024
Qubit Protein Assay kit	ThermoFisher Scientific	Cat#Q33211
Oligonucleotides		
PCR primers see Table S1	This paper	N/A
Recombinant DNA		
pZE21 plasmid	Lutz and Bujard, 1997	N/A
pZE31 plasmid	Lutz and Bujard, 1997	N/A
Software and Algorithms		
GraphPad Prism version 7.01 for Windows	GraphPad Software	http://www.graphpad.com
ClustalW	Thompson et al., 1994	http://www.clustal.org
Mega7	Kumar et al., 2016	https://www.megasoftware.net
FigTree	Rambaut, 2008	http://tree.bio.ed.ac.uk
Analyst 1.5.2	Applied Biosystems	https://sciex.com

CONTACT FOR REAGENT AND RESOURCE SHARING

Further information and requests for resources and reagents should be directed to and will be fulfilled by the Lead Contact, Gautam Dantas (dantas@wustl.edu).

EXPERIMENTAL MODEL AND SUBJECT DETAILS

Escherichia coli (DH10B and BL21(DE3)), *Haemophilus influenzae* KW20 (ATCC 51907), *Salmonella enterica* LT2 (ATCC 700720), *Enterobacter cloacae* 96-3 (ATCC 13047), and *Clostridium acetobutylicum* NCIB 8052 (ATCC 824) were cultured respectively (1) aerobically at 37°C in LB, (2) aerobically at 37°C in DSMZ *Haemophilus* medium (per liter: 21 g Mueller-Hinton broth, 5 g yeast extract, supplemented with 15 mg each of NAD and hemine), (3) aerobically at 37°C in Mueller-Hinton broth, (4) aerobically at 37°C in Mueller-Hinton broth, or (5) anaerobically at 37°C in ATCC modified reinforced Clostridial broth (per liter: 10 g tryptose, 10 g beef extract, 3 g yeast extract, 5 g dextrose, 5 g NaCl, 1 g soluble starch, 0.5 g L-cysteine HCl, 3 g sodium acetate, and 4 ml of 0.025% resazurin). For routine growth, *E. coli* strains were incubated aerobically at 37°C in LB media or in Mueller-Hinton media for antibiotic susceptibility tests with kanamycin sulfate at 50 µg/ml when appropriate. Strain identities were verified through successful amplification of target reductase genes confirmed by Sanger sequencing (see Methods Details: [Gene Amplification and Cloning](#)).

METHODS DETAILS

Gene Amplification and Cloning

Genomic DNA from grown cultures was extracted and purified using a Wizard Genomic DNA purification kit (Promega, No. A1120) according to manufacturer's instructions. *Streptococcus pyogenes* HSC5 genomic DNA was kindly provided to us by the Caparon lab at Washington University in St. Louis. Reductase and *cat* genes were amplified from genomic DNA, or the pZE31 vector ([Lutz and Bujard, 1997](#)) for *cat*, with primer pairs specified in [Table S1](#) using Platinum Pfx polymerase (ThermoFisher Scientific, No. 11708039) or Q5 hotstart 2X master mix (New England Biosciences, No. M0494L) according to manufacturer's guidelines. Inserts were purified by QIAquick PCR purification kit (Qiagen, No. 28104) and ligated into modified pZE21 ([Lutz and Bujard, 1997](#)) or pET-28b(+) (with N-terminal 6X-his tag) vectors via blunt-ended ligation using Fast-Link DNA ligation kit (Epicentre, No. LK0750H) or 2X Gibson Assembly master mix (New England Biosciences, No. E2611S). Constructs were next transformed into chemically competent *E. coli* DH10B cells (pZE21 vectors) or *E. coli* BL21(DE3) (pET-28b(+)) vectors by heat shock at 42°C followed by recovery for 30 minutes at 37°C in SOC media (Invitrogen, No. 46-0821) and plating on to LB agar with 50 µg/ml kanamycin. Colonies were picked into LB with kanamycin, grown overnight at 37°C with aeration and plasmids extracted by QIAprep Spin Miniprep kit (Qiagen, No. 27104). Insert integrity was finally verified by Sanger sequencing (Genewiz). All strains were stored long-term at -80°C as stocks in 15% glycerol in LB.

Microbroth Serial Dilution Assays

Microbroth serial dilution assays were used to determine IC₅₀ values for amphenicols and metronidazole in a modification of EUCAST standard protocol. 96-well plates (COSTAR, 3595) were prepared with 100 µl volumes of antibiotics in Mueller-Hinton broth with kanamycin arranged in two-fold dilutions by column, with concentrations ranging from 512 µg/ml to 0.5 µg/ml for chloramphenicol, 512 µg/ml to 0.25 µg/ml for metronidazole and florfenicol, or 1024 µg/ml to 0.5 µg/ml for thiampenicil (concentrations are two-fold greater than final concentrations).

Overnight Mueller-Hinton with kanamycin starter cultures of *E. coli* DH10B strains expressing reductase genes on pZE21 vectors were inoculated into fresh Mueller-Hinton with kanamycin at a density of 0.1 AU measured at 600 nm (OD₆₀₀). Diluted cultures were added to the prepared antibiotic-containing 96-well plates in 100 µl aliquots for an initial OD₆₀₀ and volume of 0.05 AU and 200 µl respectively, with each strain/antibiotic combination prepared in triplicate. After inoculation, 96-well plates were sealed with Breathe-Easy membranes (Sigma-Aldrich, Z380059) and incubated with shaking at 220 rpm at 37°C for 18 to 24 hours. Growth was measured at 600 nm in a Powerwave HT microplate spectrophotometer (Bioteck, Inc.). Dose-response curves were plotted and analyzed using GraphPad Prism version 7.01 for Windows (GraphPad Software, La Jolla California, USA). Triplicate data were fit to the following four parameter Hill equation:

$$Y = \text{Bottom} + (\text{Top} - \text{Bottom}) / \left(1 + \left(\frac{X^{\text{HillSlope}}}{IC_{50}^{\text{HillSlope}}} \right) \right)$$

IC₅₀ p-values were calculated by One-way ANOVA with Dunnett's correction for multiple comparisons. MIC was determined by taking the lowest concentration that resulted in culture growth measuring less than 0.1 AU at 600 nm. Chloramphenicol resistant/susceptible breakpoint of 8 µg/ml is according to EUCAST standards for *E. coli*.

Phylogenetic Analysis of Reductase Proteins

Amino acid sequences were downloaded and aligned using ClustalW (Thompson et al., 1994) in Mega7 (Kumar et al., 2016) using default parameters with manual trimming. Un-targeted NfsB homologs were downloaded from the UniProt database (UniProt Consortium, 2015). The resulting alignment was used to construct a Maximum Likelihood tree with default parameters and 100 rounds of bootstrapping in Mega7. The tree was visualized in the tree viewing program FigTree (Rambaut, 2008).

Lag-Phase Chloramphenicol Modification Assay

Triplicate 100 µl aliquots of LB with kanamycin and 0 µg/ml, 8 µg/ml, 16 µg/ml, 32 µg/ml, 64 µg/ml, or 128 µg/ml chloramphenicol were prepared in a 96-well plate (COSTAR, 3595). Overnight triplicate cultures of empty vector or *H. influenzae nfsB*-expressing *E. coli* cultures were grown in LB with kanamycin and diluted 10-fold into fresh LB with kanamycin and incubated for 3 hours at 37°C in order to enter exponential phase. Exponentially growing cultures were diluted to an OD₆₀₀ of 0.1 AU and added in 100 µl volumes to the 96-well plate. Plates were sealed as before and incubated in a Powerwave HT microplate spectrophotometer (Biotek, Inc.) at 37°C with constant shaking (medium setting, rpm not available) for 96 hours with monitoring every 30 minutes. Growth data were fit to the Hill equation as above to determine how many hours of incubation were required to reach half-maximal growth. A plot of chloramphenicol concentration against time to reach 50% growth was prepared and projected to 96 hours.

Pre-conditioned Media Assay

E. coli containing empty pZE21 vector or vector-expressed *H. influenzae nfsB* were inoculated into LB with kanamycin and 8 µg/ml chloramphenicol and incubated overnight at 37°C alongside a cell-free (+) chloramphenicol control and an empty vector (-) chloramphenicol control. Following overnight growth cells were removed from cultures by first pelleting at 16,000 rcf for 10 minutes, followed by filtration of the supernatant through a 0.22 µm filter. Cell-free supernatants were split into three aliquots as technical replicates and inoculated with *E. coli* containing empty vector (to provide resistance to residual kanamycin) prior to incubating overnight at 37°C. Following incubation growth was measured as before and OD₆₀₀ values were compared using a one-way ANOVA test with Dunnett's correction for multiple comparisons to determine level of chloramphenicol removal in the pre-conditioned media.

H. influenzae NfsB Expression and Purification

E. coli BL21(DE3) containing pET-28b(+) with *H. influenzae nfsB* open reading frame downstream of a 6-histidine tag was inoculated into 3 ml Studier auto-inducing media ZYM-5052 (Studier, 2005) with kanamycin and grown overnight with aeration at 37°C. 750 µl aliquots of grown culture were added a 750 ml culture of ZYM-5052 with 100 µg/ml kanamycin and to three 750 ml cultures of Terrific broth (TB, Fisher Scientific, No. BP9729-600) supplemented with 2 mM MgSO₄ in 2.8 L Fernbach flasks. Cultures were shaken at 350 rpm at 37°C in a MaxQ 5000 (Thermo Scientific) temperature-controlled incubator until OD₆₀₀ of ~1 was reached (~3 hour incubation). The incubator temperature was reduced to 25°C and the TB flasks were induced with 0 µM, 100 µM, or 250 µM IPTG with shaking for 48 hours with aliquots taken at 24 hours as well. Cell aliquots taken at 24 hours and 48 hours were pelleted at 8,000 rcf, resuspended in phosphate buffered saline (PBS), and 100 µl aliquots were lysed by sonication using a Bioruptor Pico (Diagenode) at 4°C for 10 minutes with 30 seconds on and 30 seconds off. Lysates were centrifuged at 21,000 rcf to separate soluble and insoluble fractions and analyzed for soluble enzyme production via SDS-PAGE analysis with Sypro Ruby gel stain (ThermoFisher, No. S12001). While 24 hour incubation in ZYM-5052 gave the best results, the 48 hour incubations for all four flasks were combined and cells pelleted at 8,000 rcf for 20 minutes using a Sorvall Legends XTR centrifuge (Thermo Scientific) in a Fiberlite F14-6x250 LE rotor (Thermo Scientific) before removal of supernatants and freezing of wet cell pellets overnight at -80°C.

Cell pellets were weighed and allowed to thaw on ice. All following steps were performed at 4°C or on ice. The cell pellets were resuspended to 20% w/v in ice-cold loading buffer consisting of (per liter) 8.709 g K₂HPO₄ (50 mM), 29.22 g NaCl (500 mM), 351 µl β-mercaptoethanol (5 mM), 0.68 g imidazole (10 mM), and 100 ml glycerol (10% v/v) at pH 8 with addition of lysozyme at 1 mg lysozyme/g wet cell mass. Suspensions were incubated on ice for 30 minutes then lysed by sonication on a Branson Sonifier 250 instrument (Branson Ultrasonics) with microtip adjusted to reach ca. 30% output on 50% duty until suspension viscosity and color were reduced. Insoluble matter was clarified from the suspensions by centrifugation for 30 min at 24,446 rcf at 4°C in a Sorvall Legends XTR centrifuge (Thermo Scientific) in a Fiberlite F15-8x50 cy rotor (Thermo Scientific). Supernatants were collected and stored at 4°C until purification.

Purification of the His-tagged enzyme was performed using an Ni-NTA nickel resin (BioRad, No. 7800800) and a low-pressure chromatography system (BioRad, Econo system) coupled to a fraction collector (BioRad, No. 7318122) as previously described (Crofts et al., 2018). Fractions containing purified enzyme were identified by their yellow color and verified by SDS-PAGE analysis and staining with Bio-Safe Coomassie stain (BioRad, No. 1610796) according to manufacturer's instructions. Fractions containing pure recombinant *H. influenzae NfsB* were pooled and concentrated via centrifugation through a 10 kDa molecular weight cut-off filter (Amicon, No. UFC901024) according to manufacturer's instructions. The ca. 1 ml concentrate was washed three times as above with storage buffer consisting of (per liter) 8.709 g K₂HPO₄ (50 mM), 8.766 g NaCl (250 mM), 1 ml of 1 M dithiothreitol (1 mM) and 50 ml of glycerol (5% v/v) at pH of 7.5. Purified enzyme concentration was determined by Qubit Protein Assay kit (Thermo Scientific, No. Q33211) and the mass concentration was converted to molar concentration using molecular weights predicted by EXPASY (Gasteiger et al., 2003). Aliquots of 55 µl were stored at -80°C.

Chloramphenicol Reduction Assay Optimization

A preliminary *in vitro* assay based on reported reductase conditions (Mermod et al., 2010; Smith et al., 2007) demonstrated that the *H. influenzae* NfsB enzyme could reduce chloramphenicol (see below for optimized conditions). We used these baseline conditions to determine the effect of reduced cofactor on activity. A pre-reaction mixture was prepared containing 50 mM Tris-HCl pH 8, 2 mM chloramphenicol, 10 μ M flavin mononucleotide (FMN), and 1 μ M *H. influenzae* NfsB. Six 100 μ l aliquots were transferred to a 96-well plate (COSTAR, 3595) to which was added 100 μ l of 2 mM NADH (Grainger, No. 31GA86) or NADPH (Cayman chemical, No. 9000743) in 50 mM Tris-HCl pH 8. Oxidation of NAD(P)H to NAD(P)⁺ was monitored at 340 nm (Mermod et al., 2010) for 30 min at 25°C in a Powerwave HT microplate spectrophotometer (Bioteck, Inc.) with minimal kinetic interval.

In order to determine the identity of the native flavin cofactor, a 50 μ l aliquot of enzyme was heated at 70°C for 20 minutes to denature the enzyme and release the tightly bound flavin (Zenno et al., 1996b). The yellow supernatant was removed following centrifugation at 21,000 rcf for 20 min and analyzed via thin layer chromatography using silica gel 60 F₂₅₄ (Millipore Sigma, No. 105794) alongside standards and extract/standard co-spots in a solvent system consisting of 5:2:3 1-butanol:acetic acid:H₂O (Sherma and Fried, 2003). The plate was visualized and photographed under UV-vis at 366 nm in a Gel-Doc XR+ (BioRad). The observed retention factors of the standards were consistent with the literature.

To determine optimal pH for *H. influenzae* NfsB activity 100 mM Tris/citrate buffer with 10 μ M FMN and 2 mM chloramphenicol was prepared. 400 μ l aliquots of buffer were prepared at pH values ranging from 3 to 9 and aliquoted as seven technical replicates in 100 μ l volumes in a 96-well plate (COSTAR, 3595). A second solution containing 1 μ M enzyme and 6 mM NADPH was prepared and added in 100 μ l volume to all buffer wells. Reactions were monitored at 340 nm as before and the progress curve slopes were compared to determine relative activity compared to the most active samples in GraphPad Prism (GraphPad Software, La Jolla California, USA). Due to the highly variable nature of the assay, Grubbs test with $\alpha=0.2$ for outlier detection was used to remove potentially inaccurate samples.

To determine appropriate temperature ranges for enzyme activity, substrate mixes of 50 mM Tris-HCl pH 8, 1.25 mM NADPH, 1.25 mM chloramphenicol, and 6.25 μ M FMN were aliquoted 40 μ l at a time into PCR tubes (four replicates for each temperature to be tested). Substrate mixes were pre-incubated in a thermocycler at the test temperature for 1 minute following which 10 μ l of enzyme solution (2.5 μ M in 50 mM Tris-HCl pH 8) was added. Reactions were allowed to incubate for 4 minutes at which point they were quenched by addition of 50 μ l of 20% trichloroacetic acid (TCA) and transfer to ice. Reaction progress was measured in quenched samples by derivatization of amino-chloramphenicol by the Bratton-Marshall method (Bratton and Marshall, 1939; Smith et al., 2007). Briefly, 12.5 μ l of the following solutions were added sequentially with 10 minute incubations at room temperature: 0.1% sodium nitrite, 0.5% ammonium sulfamate, and 0.05% Bratton-Marshall reagent (N-(1-Naphthyl)ethylenediamine dihydrochloride, 20 minutes). The reactions were then transferred to half-area 96-well plates (Corning, No. 3696) and Abs₅₅₀ measurements were taken using a Powerwave HT microplate spectrophotometer (Bioteck, Inc.) to quantify production of aryl-amines. Absorbance at 550 nm was normalized as percent maximum for each reaction and outliers were excluded using a Grubbs test with $\alpha=0.2$. All following reactions were performed in 50 mM Tris-HCl at pH 8 and at 25°C unless otherwise stated.

Chloramphenicol Modification LCMS Assay

Enzymatic loss of chloramphenicol during NfsB reduction was monitored by liquid chromatography tandem mass spectrometry (LCMS) as follows. Two 700 μ l aliquots of substrate buffer consisting of 2 mM NADPH, 10 μ M FMN, and 600 μ M chloramphenicol were prepared. An equal volume of Tris buffer or 1 μ M enzyme in Tris buffer was added to each aliquot at t=0 and 250 μ l was immediately removed and quenched with 12 μ l of 88% formic acid. Additional 250 μ l aliquots were quenched at 2.5 min, 5 min, 7.5 min, and 10 min.

Samples were sent to the Metabolomics Facility at Washington University for LCMS analysis where they were diluted 5-fold in methanol. An equal volume of 10 μ g/ml thiamphenicol as internal standard was added to each sample before loading onto an ACE Excel Super C18 column (3 μ m, 50 x 4.6 mm) on an Applied Biosystems Sciex 4000QTRAP tandem mass spectrometer. Samples were run with multiple reaction monitoring (MRM) in negative mode. Chloramphenicol standards were used to prepare calibration curves in duplicate for quantification.

Amino-Chloramphenicol Detection Assay

The product of *H. influenzae* NfsB reduction of chloramphenicol in the presence of excess reducing equivalence was analyzed by targeted LCMS. Amino-chloramphenicol HCl salt was purchased from Toronto Research Chemicals (No. A622670) as a standard. An NADPH regeneration system (Xenotech, No. K5000) was used according to the manufacturer's protocols to provide the equivalent of 700 μ M to 900 μ M NADPH concentrations during an overnight reaction. The reaction consisted of the regeneration system, 2 mM chloramphenicol, 15 μ M FMN, and ca. 1.5 μ M enzyme dissolved in 35 ml of 50 mM Tris-HCl buffer. Following incubation for 22.5 hours at room temperature the reaction was extracted three times with 10 ml of ethyl acetate. The combined organic layers were extracted three times with 2.5 ml of 0.1 M aqueous HCl. The aqueous extracts were combined, frozen at -80°C, and lyophilized to dryness. The dried yellow product was dissolved in 750 μ l water and checked for potential presence of amino-chloramphenicol by Bratton-Marshall derivatization and TLC analysis against an amino-chloramphenicol standard (silica, 8:2 dichloromethane:methanol, visualized with iodine vapour).

LCMS analyses were performed at the Metabolomics Facility at Washington University on an Applied Biosystems Sciex 4000QTRAP tandem mass spectrometer coupled to a Shimadzu 20AD HPLC system. Metabolites were separated using an ACE

Excel 3 super C18 column (3 μm , 50 x 4.6 mm) running 0.03% diethylamine and 20 mM hexafluoro-2-propanol in water, pH 8.5 (solvent A) against methanol (solvent B). The full mass scan (Q3 scan) and MS2 scans of m/z 291 (amino-chloramphenicol) and m/z 321 (chloramphenicol) were acquired for the samples as well as amino-chloramphenicol and chloramphenicol standards. Data processing was conducted with Analyst 1.5.2 (Applied Biosystems).

Enzyme Substrate Specificity and Activity

Reactions to examine substrate activity and specificity were set-up by preparing substrate mixes containing 2 mM NADPH and 10 μM FMN and each substrate in triplicate. Concentrations (at twice the final reaction concentration) ranged from 3 mM to 46.875 μM (chloramphenicol, thiamphenicol, florfenicol, 3-nitrophenol, and 4-nitrophenol), 750 μM to 46.875 μM (metronidazole), and 1.5 mM to 46.875 μM (menadione) by 2-fold steps and were prepared as 50 μl aliquots in a half-area 96-well plate (Corning, No. 3696). Enzyme solution was prepared at 1 μM , and 50 μl of enzyme solution was added to all wells with mixing, followed by monitoring of the reaction progression in a Powerwave HT microplate spectrophotometer (Biotek, Inc.) with minimal kinetic interval at 340 nm for NADPH oxidation (chloramphenicol, thiamphenicol, florfenicol, metronidazole, menadione, and 3-nitrophenol), or at other wavelengths when spectra interfered substantially with measurements at 340 nm (420 nm for nitrofurantoin, 450 nm for 4-nitrophenol). In some cases (metronidazole and menadione) an optimal wavelength could not be found resulting in the exclusion of high substrate concentration data points where spectral overlap was too high.

Initial rate velocities in absorbance change, found by taking the slope during the linear stage of the reactions, were converted to $\mu\text{M s}^{-1}$ using automatic pathlength correction and the following extinction coefficients for the substrate being monitored (determined empirically in triplicate if needed): NADPH $\epsilon_{340}=6220 \text{ M}^{-1} \text{ cm}^{-1}$ (Mermod et al., 2010), nitrofurantoin $\epsilon_{420}=7970 \text{ M}^{-1} \text{ cm}^{-1}$, and 4-nitrophenol $\epsilon_{450}=3211 \text{ M}^{-1} \text{ cm}^{-1}$. Triplicate data points were plotted in GraphPad Prism (GraphPad Software, La Jolla California, USA) and fit to Michaelis-Menten curves for k_{cat} and K_M determination using the following equation:

$$Y = Et * k_{cat} * X / (K_M + X)$$

Where Et corresponds to enzyme concentration (0.5 μM). For each fit the estimated 95% confidence interval as well as K_M were plotted on the graph while k_{cat} values were recorded elsewhere.

In order to monitor chloramphenicol nitro group reduction three assays were performed. In the first assay, 100 μl reactions arrayed in 8 replicates containing 50 mM Tris-HCl buffer at pH 8, 1 mM NADPH, 50 μM FMN, 5 μM enzyme, and 250 μM substrate were allowed to react for 30 minutes at room temperature along with control reactions lacking substrate or NADPH. Substrates included chloramphenicol, metronidazole, nitrofurantoin, 3-nitrophenol, and 4-nitrophenol. Following incubation, reactions were quenched with an equal volume of 20% TCA and analyzed by Bratton-Marshall assay (see previous section for method). In the second assay, four reactions in triplicate containing ca. 2 mM NADPH, 5 μM FMN, 0.5 μM enzyme, and 1 mM, 333 μM , 111 μM , or 37 μM chloramphenicol were allowed to proceed with an aliquot being removed at t=0, 1, 2, 3, and 4 minutes into an equal volume of 20% TCA for Bratton-Marshall derivatization as performed earlier. The absorbance at 550 nm was plotted to demonstrate accumulation of amino-chloramphenicol over time, with increased accumulation at higher chloramphenicol concentrations. In the third assay, 200 μl reactions in a UV transparent 96-well plate (Corning, No. 3635) containing 0.5 mM NADPH, 0.5 mM chloramphenicol, and 0.25 μM enzyme, or with each ingredient missing, were monitored at 340 nm for NADPH oxidation to NADP⁺ and at 282 nm (the isosbestic point of NADPH/NADP⁺) for loss of the chloramphenicol nitro group with minimal interval on a Powerwave HT microplate spectrophotometer (Biotek, Inc.).

Checkerboard Assay to Detect Synergy

Triplicate 96-well plates (COSTAR, 3595) were prepared containing 100 μl of Mueller-Hinton broth with kanamycin and mixtures of chloramphenicol and metronidazole. Chloramphenicol ranged in concentrations from 512 $\mu\text{g/ml}$ to 0.25 $\mu\text{g/ml}$ by 2-fold jumps and metronidazole ranged in concentrations from 1024 $\mu\text{g/ml}$ to 0.125 $\mu\text{g/ml}$ by 4-fold jumps, with each chloramphenicol concentration existing as a mixture with each metronidazole concentration. *E. coli* expressing *H. influenzae nfsB* or containing empty vector were inoculated into Mueller-Hinton broth with kanamycin and incubated overnight with aeration at 37°C. The resulting cultures were diluted in Mueller-Hinton broth with kanamycin to an OD₆₀₀ of 0.1 AU and added as 100 μl aliquots to the wells of the prepared antibiotics plates. Plates were sealed as before and incubated at 37°C with shaking for 20 to 24 hours before measuring OD₆₀₀ as above. Chloramphenicol growth inhibition at each metronidazole concentration was analyzed using GraphPad Prism (GraphPad Software, La Jolla California, USA) as before. Fractional inhibitory concentration indices (FICI scores) were calculated following growth by scoring wells with OD₆₀₀ less than 0.1 AU as inhibited. FICI scores of <1 were taken as evidence for synergistic relationships, near 1 as additive, and >1 as antagonistic.

In Vitro Inhibition of Chloramphenicol Reduction

Substrate buffer was prepared with 2 mM NADPH, 10 μM FN, and 982 μM (twice the measured K_M). Inhibitors metronidazole and dicoumarol were prepared in substrate buffer and added in triplicate to a UV transparent 96-well plate (Corning, No. 3635) in 50 μl aliquots with metronidazole ranging in concentration from 4096 $\mu\text{g/ml}$ to 2 $\mu\text{g/ml}$ and dicoumarol ranging in concentration from 1024 $\mu\text{g/ml}$ to 1 $\mu\text{g/ml}$ by 2-fold jumps. *H. influenzae NfsB* was prepared at 1 μM in Tris buffer and 50 μl aliquots were added with mixing prior to monitoring of chloramphenicol reduction at 281 nm on a Powerwave HT microplate spectrophotometer (Biotek,

Inc.) with minimal interval. Velocities were normalized against wells containing no inhibitor, and inhibition dose-response curves were determined as before using GraphPad Prism (GraphPad Software, La Jolla California, USA) to find IC₅₀ concentrations.

QUANTIFICATION AND STATISTICAL ANALYSIS

For all assays, replicate descriptions are available in the corresponding methods section as well as in the specific figure legend. Statistical analyses were carried out using GraphPad Prism with experiment-specific details available in the corresponding methods section and figure legend.

Supplemental Information

**Discovery and Characterization of a Nitroreductase
Capable of Conferring Bacterial
Resistance to Chloramphenicol**

Terence S. Crofts, Pratyush Sontha, Amber O. King, Bin Wang, Brent A. Biddy, Nicole Zanolli, John Gaumnitz, and Gautam Dantas

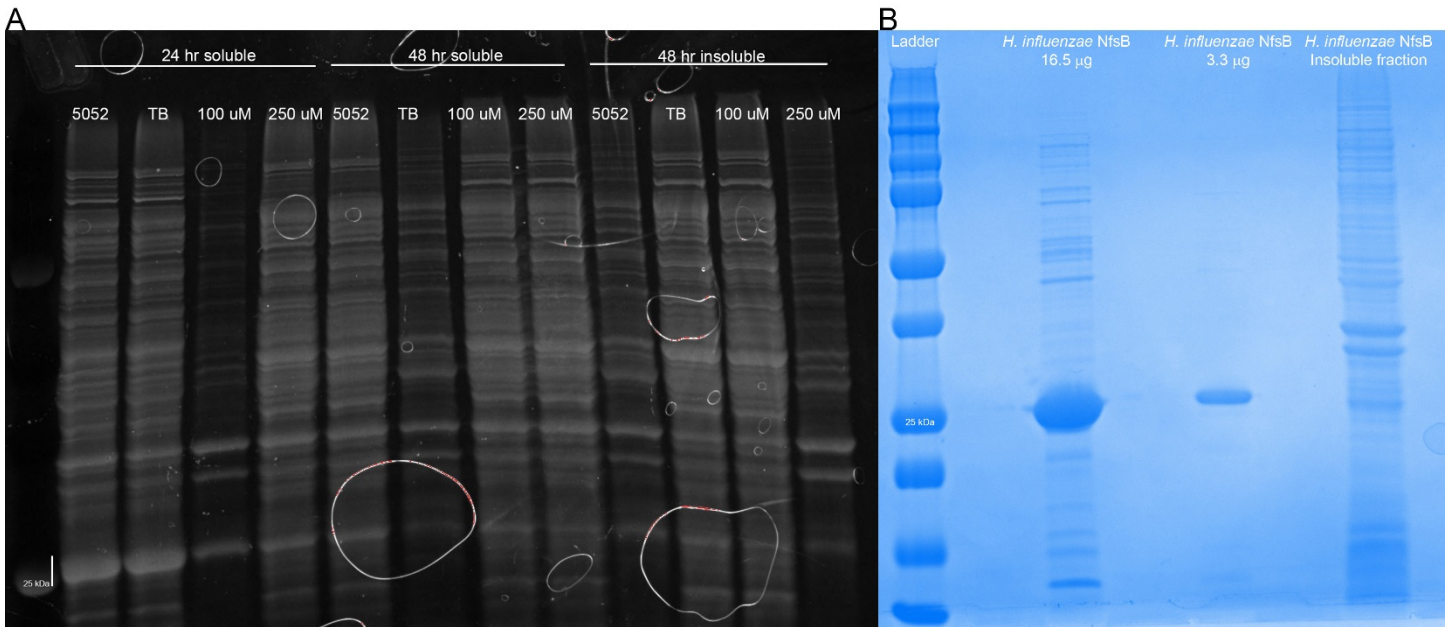
Supplemental table 1. Primers for gene amplification. Related to Star★Methods section METHODS DETAILS: Gene amplification and cloning.

Organism/Source	Citation	Forward primer	Reverse primer
<i>H. influenzae</i> DSM 11121	(Smith et al., 2007)	ATGACTCAACT TACTCGTGAAC AAG	TTACCCCCACCC ATTTCACC
<i>S. pyogenes</i> HSC5	(Egami et al., 1951)	ATGAAATTCT AGAGTTAAACA AAAAACG	CTATCTTCTTTC GATGACTTCAT CAAC
<i>E. coli</i> BL21(DE3)	(Smith and Worrel, 1953)	ATGGATATCAT TTCTGTGCCCTT AAAG	TTAGACTTCGGT TAAGGTGATGT TTTG
<i>E. cloacae</i> ATCC 13047	(Bryant and DeLuca, 1991)	ATGGATATTATT TCTGTCGC	TTAGCACTCAG TCACAATCGT
<i>S. enterica</i> ATCC 700720	(Yanto et al., 2010)	ATGGATATCGT TTCTGTGCCCTT	TTAAACTTCCGT CAGTGTGGTT
<i>C. acetobutylicum</i> ATCC 824	(O'Brien and Morris, 1971; Onderdonk et al., 1979)	ATGCTTAAAGA GATAGAAGAAA G	TCACCATTTC CATATGAATTAA
<i>cat</i> from pZE31	(Lutz and Bujard, 1997)	ATGGAGAAAAA AATCACTGGAT ATACC	TTACGCCCGC CCTG

Supplemental table 2. Michaelis-Menten kinetics constants of *H. influenzae* NfsB reduction reactions. Related to figure 6.

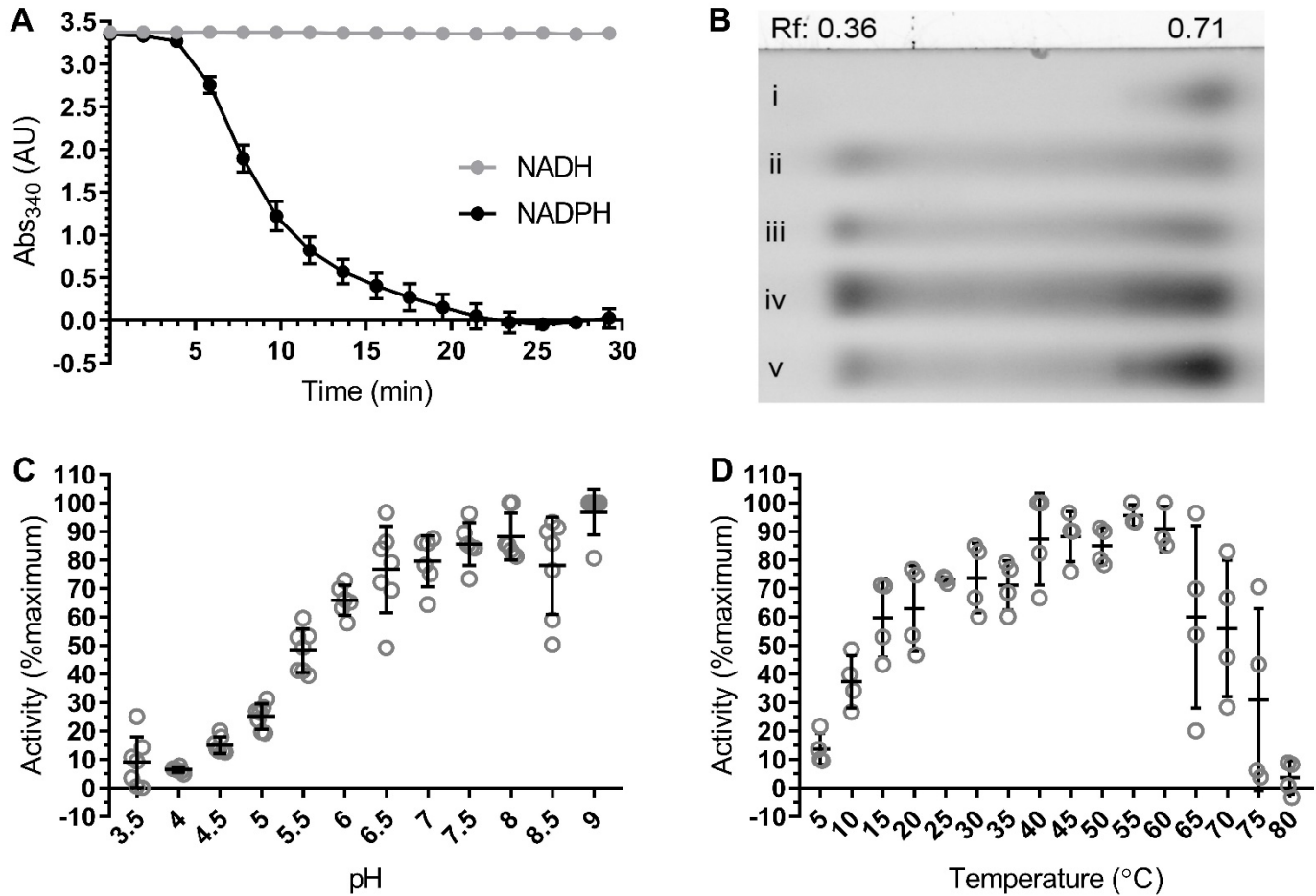
Substrate	k_{cat} (s ⁻¹)	95% CI	K _M (μM)	95% CI	k_{cat}/K_M (mM ⁻¹ s ⁻¹)
Chloramphenicol	10.2	9.42 - 11.0	491	409 - 593	20.7
Thiamphenicol	nd	nd	nd	nd	nd
Florfenicol	nd	nd	nd	nd	nd
Metronidazole	0.337	0.268 - 0.435	73.8	36.9 – 143	4.57
Nitrofurantoin	9.43	7.50 - 11.7	38.8	15.1 - 83.7	242
Menadione	12.1	9.74 - 15.3	152	85.4 – 277	79.3
3-Nitrophenol	4.31	3.97 - 4.66	69.7	50.7 - 94.4	61.8
4-Nitrophenol	≥0.03	nd	≥750	nd	nd

nd: Not determined



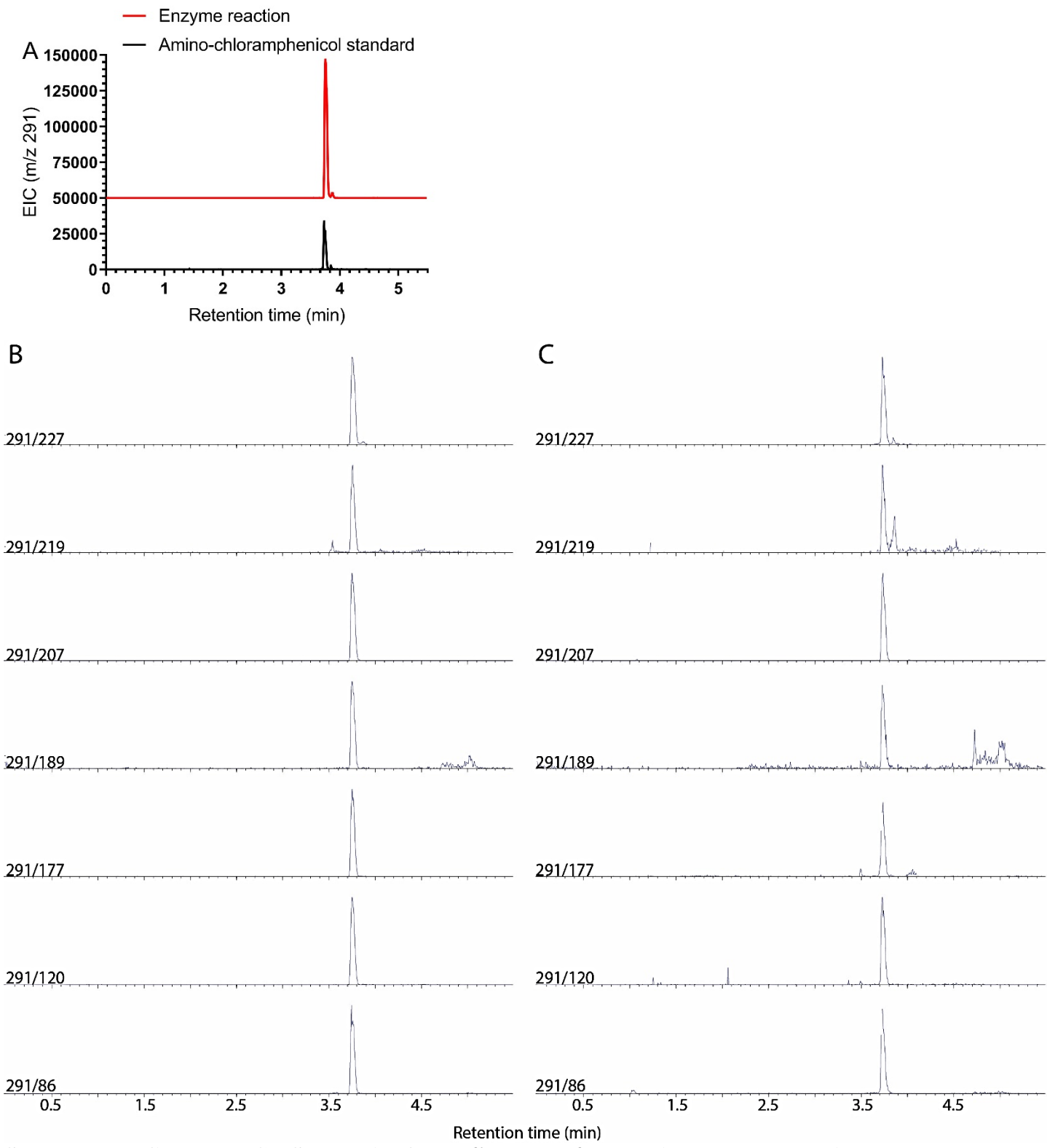
Supplemental figure 1. Expression and purification of *H. influenzae* NfsB from *E. coli*. Related to Figure 5.

(A) Sypro Ruby SDS-PAGE gel analysis of culture conditions for optimal production of soluble *H. influenzae* NfsB from *E. coli*. 5052 corresponds to Studier auto-induction media ZYM-5052, TB stands for terrific broth, and 100 µM and 250 µM correspond to TB with the indicated concentrations of IPTG added for induction. The 25 kDa ladder is labelled on the left and a vertical white line indicates the expected migration distance for the protein of interest. (B) Coomassie stained SDS-PAGE gel of final purified *H. influenzae* NfsB at two dilutions as well as undiluted insoluble protein fraction. The 25 kDa marker on the ladder is highlighted. See also figure 5.



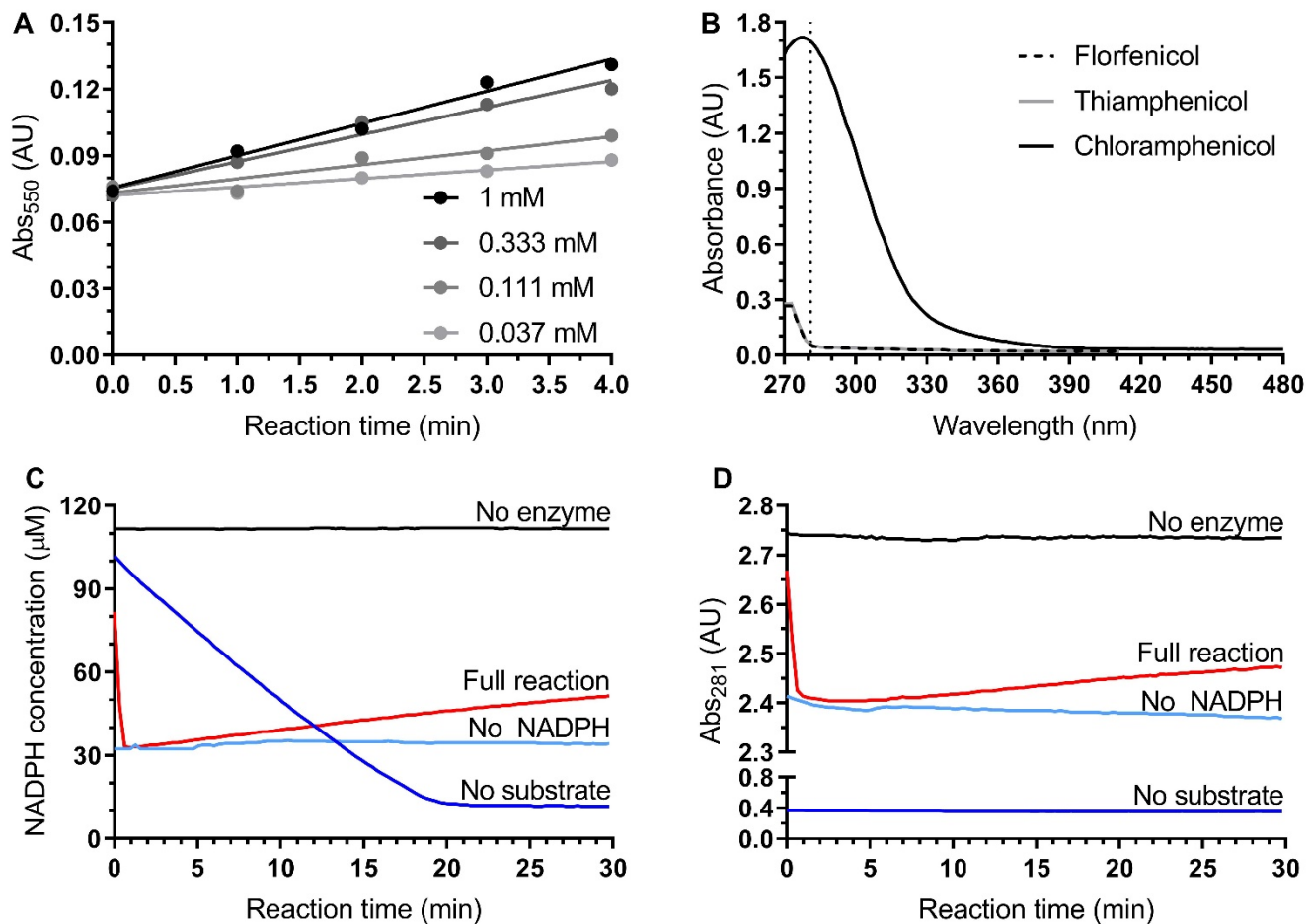
Supplemental figure 2. *H. influenzae* NfsB physiological requirements. Related to Figure 5.

(A) Assay to determine preferred cofactor for *H. influenzae* NfsB. Reactions compared 1 mM NADP against 1 mM NADPH and monitored cofactor oxidation at 340 nm. Data represents mean values of three replicates and error bars display the standard deviation. (B) TLC analysis of (i) riboflavin, (ii) flavin mononucleotide, (iii) extract from denatured NfsB, (iv) co-spot of flavin mononucleotide and NfsB extract, and (v) co-spot of riboflavin and NfsB extract. Solvent consisted of 5:2:3 butanol:acetic acid:water and TLC was visualized under UV light. (C) Graph of normalized reaction velocities against pH with seven replicates and standard deviation. Outliers were removed by Grubbs test with $\alpha = 0.2$. (D) Graph of normalized Bratton-Marshall derivitizable compounds produced by reactions quenched after four minutes at the given temperature. Displayed are the mean and standard deviations of four replicates, with outliers removed by Grubbs test with $\alpha = 0.2$. See also figure 5.



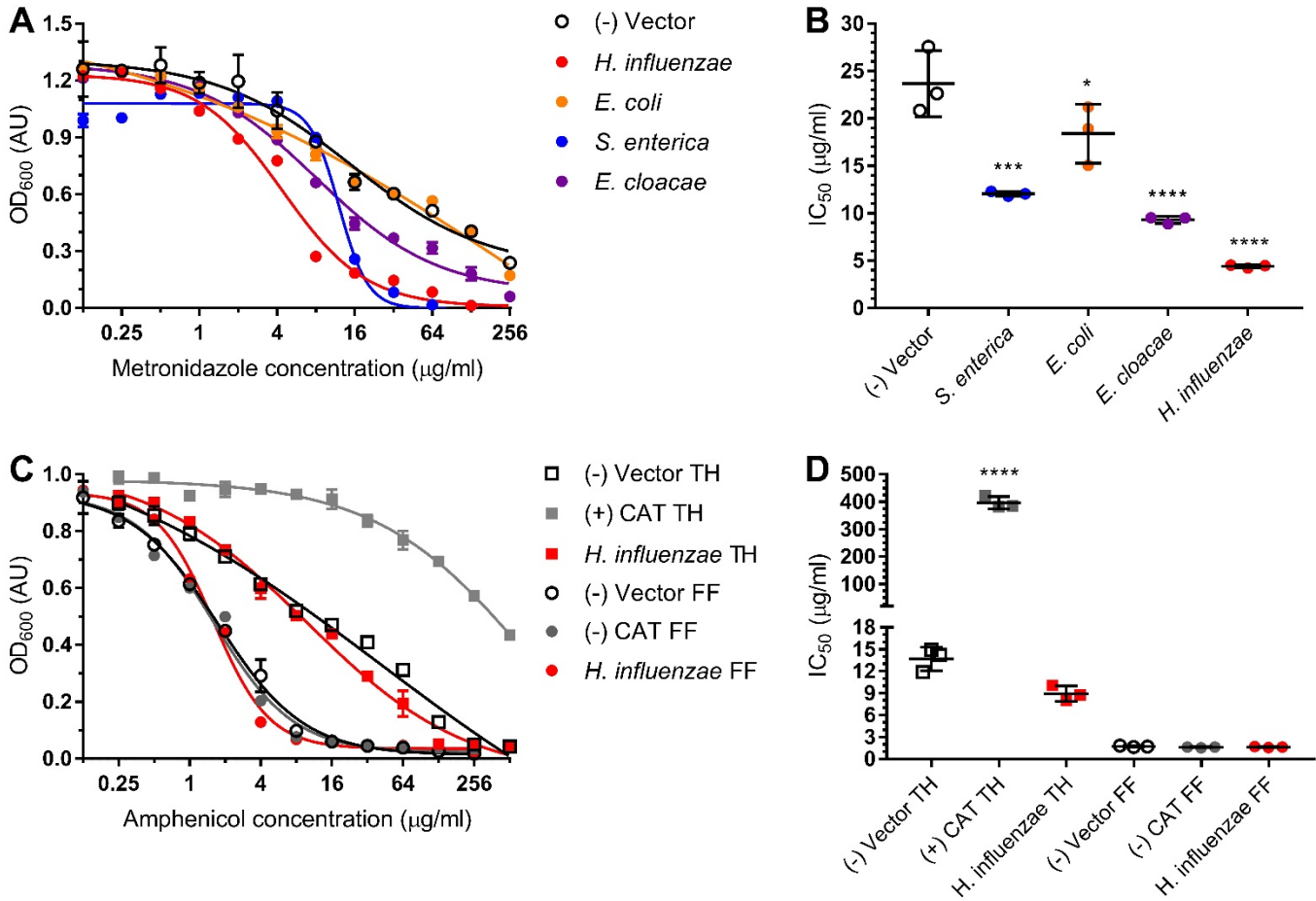
Supplemental figure 3. LCMS analysis of *H. influenzae* NfsB reactions. Related to Figure 5.

(A) LCMS extracted ion count analysis (291 m/z, corresponding to amino-chloramphenicol) of representative reaction (red) compared to amino-chloramphenicol standard (black). (B-C) Multiple-reaction monitoring (MRM) LCMS of (B) amino-chloramphenicol standard and (C) reaction product with the indicated precursor and product ions (e.g. 291 m/z precursor, 86 m/z product). See also figure 5.



Supplemental figure 4. Alternative methods for following the *H. influenzae* NfsB reduction of chloramphenicol. Related to Figure 6.

(A) Bratton-Marshall detection of aryl amines of *H. influenzae* NfsB reaction with 1 mM, 0.333 mM, 0.111 mM, and 0.037 mM chloramphenicol after 1 minute, 2 minutes, 3 minutes, and 4 minutes. (B) UV-vis spectra of 1 mM solutions of chloramphenicol, thiamphenicol, and florfenicol in 50 mM Tris HCl at pH 8. The dotted vertical line corresponds to 281 nm. Reaction monitoring for (C) oxidation of NADPH to NADP⁺ or (D) reduction of the chloramphenicol nitro group in full enzyme reactions (red), and reactions individually lacking enzyme (black), chloramphenicol (blue) or NADPH (teal). See also figure 6.



Supplemental figure 5. Reductase expression alters susceptibility of *E. coli* to metronidazole but not nitro-lacking amphenicols. Related to figures 2 and 7.

Dose-response curves of microbroth dilution assays for *E. coli* expressing predicted reductase gene homologs in the presence of (A) metronidazole or (C) semi-synthetic amphenicols (thiamphenicol TH, florfenicol FF) with respective 50% inhibitory concentrations (IC₅₀) calculated from the curve fit (B and D). All points are averages of triplicate experiments with standard deviation error bars. Statistical significance was calculated with respect to the vector control by ordinary one-way ANOVA with Dunnett's correction for multiple comparisons. Adjusted p-value displayed as p≤0.0001 (****), p<0.001 (**), and p<0.05 (*). Abbreviation: TH, thiamphenicol; FF, florfenicol. See also figure 2 and figure 7.